Exploring the crystallization landscape of cadmium bis(*N*-hydroxyethyl, *N*-isopropyldithiocarbamate), $Cd[S_2CN(iPr)CH_2CH_2OH]_2$

Yee Seng Tan,[I] Siti Nadiah Abdul Halim[I] and Edward R. T. Tiekink*[I,II]

[I] University of Malaya, Department of Chemistry, 50603 Kuala Lumpur, Malaysia

[II] Sunway University, Centre for Chemical Crystallography, Faculty of Science and Technology, 47500 Bandar Sunway, Selangor Darul Ehsan, Malaysia

Received; accepted

Keywords: Dithiocarbamate / cadmium / supramolecular isomerism / crystal structure analysis / X-ray diffraction

Abstract. Crystallization of $Cd[S_2CN(iPr)CH_2CH_2OH]_2$ from ethanol yields the coordination polymer $[\{Cd[S_2CN(iPr)CH_2CH_2OH]_2\}\cdot EtOH]_\infty$ (**1**) within three hours. When the solution is allowed to stand for another hour, the needles begin to dissolve and prisms emerge of the supramolecular isomer (SI), binuclear $\{Cd[S_2CN(iPr)CH_2CH_2OH]_2\}_2\cdot 2EtOH$ (**2**). These have been fully characterized spectroscopically and by X-ray crystallography. Polymeric **1** has 2-fold symmetry and features dithiocarbamate ligands coordinating two octahedral Cd atoms in a $\mu_2\kappa^2$-tridentate mode. Binuclear **2** is centrosymmetric with two ligands being $\mu_2\kappa^2$-tridentate as for **1** but the other two being κ^2-chelating leading to square pyramidal geometries. The conversion of the kinetic crystallization product, **1**, to thermodynamic **2** is irreversible but transformations mediated by recrystallization (ethanol and acetonitrile) to related literature SI species, namely coordination polymer $[\{Cd[S_2CN(iPr)CH_2CH_2OH]_2\}_3\cdot MeCN]_\infty$ and binuclear $\{Cd[S_2CN(iPr)CH_2CH_2OH]_2\}_2\cdot 2H_2O\cdot 2MeCN$, are demonstrated, some of which are reversible. Three other crystallization outcomes are described whereby crystal structures were obtained for the 1:2 co-crystal $\{Cd[S_2CN(iPr)CH_2CH_2OH]_2\}_2$:2[3-(propan-2-yl)-1,3-oxazolidine-2-thione] (**3**), the salt co-crystal $[iPrNH_2(CH_2CH_2OH)]_4[SO_4]_2\{Cd[S_2CN(iPr)CH_2CH_2OH]_2\}_2$ (**4**) and the salt $[iPrNH_2(CH_2CH_2OH)]\{Cd[S_2CN(iPr)CH_2CH_2OH]_3\}$ (**5**). These arise as a result of decomposition/oxidation of the

dithiocarbamate ligands. In each of **3** and **4** the binuclear $\{Cd[S_2CN(iPr)CH_2CH_2OH]_2\}_2$ SI, as in **2**, is observed strongly suggesting a thermodynamic preference for this form.

* Correspondence author: edward.tiekink@gmail.com (E.R.T.T.)

Introduction

Contemporary applications, e.g. medicinal [1] and as single source precursors for nanoparticle generation of chalcogenides [2], complement well established uses, e.g. as lubricants, in the vulcanization of rubber, as flotation agents, etc. [3-5] of metal 1,1-dithiolates comprising ligands such as dithiocarbamate ($^-S_2CNR_2$), xanthate (^-S_2COR), and dithiophosphate [$^-S_2P(OR)_2$]. Therefore, it is not surprising that a vast amount of structural data for this class of compound exists as summarized in a number of bibliographic reviews [6-10]. These prove that an enormous range of structures have been characterized, ranging from zero- to three-dimensional architectures, and their adoption often rationalized in terms of the role of steric bulk of the remote substituents in mitigating secondary M···S interactions [11, 12], offering a new paradigm in the design of supramolecular assembly [13-16]. In the context of the present study, the structural diversity of these systems is very well illustrated in the binary cadmium xanthates, $Cd(S_2COR)_2$, where zero- (mononuclear) [17], one- [18] and two-dimensional [19-24] aggregation patterns are observed, depending on the bridging propensity of the xanthate ligands. For the cadmium dithiophosphates both zero- (binuclear) [25-27] and one-dimensional [28-30] aggregation is found. By contrast to this diversity, the structural chemistry of cadmium dithiocarbamates is remarkably less varied. In the almost 50 years since the original report of the crystal structure of binuclear $[Cd(S_2CNEt_2)_2]_2$ [31], a large number of related dialkyl species have been described as having the same binuclear structural motif, i.e. with two each of κ^2-chelating and $\mu_2\kappa^2$-tridentate dithiocarbamate ligands leading to penta-coordinate geometries, regardless of whether the R groups were the same [31-44], dissimilar [39, 45], incorporated within a cyclic system [46-49], or whether the compound was co-crystallised with another species [35, 39, 47], or that the R group carried additional potential oxygen donor atoms [44, 49]. However, this situation changed in 2013 with the report of a coordination polymer, $[\{Cd[S_2CN(iPr)CH_2CH_2OH]_2\}_3\cdot MeCN]_\infty$ [50]. Further diversity was described in 2014 with the report of a centrosymmetric trinuclear species having an octahedrally coordinated cadmium centre flanked by two square pyramidal centres [51]. For completeness, it is noted that the non-alkyl species, $\{Cd[S_2CN(H)R]_2\}_\infty$ R = *n*-C_5H_{11} and *n*-$C_{12}H_{25}$, are linear coordination polymers with octahedrally coordinated cadmium atoms [52].

The linear polymeric $[\{Cd[S_2CN(iPr)CH_2CH_2OH]_2\}_3\cdot MeCN]_\infty$ structure was of particular interest as when it was allowed to stand in the

mother liquor over a period of several days it transformed to $\{Cd[S_2CN(iPr)CH_2CH_2OH]_2\}_2 \cdot 2H_2O \cdot 2MeCN$, which has the normally adopted binuclear motif [50]. The conversion from the polymer to dimeric form was proposed to be mediated by adventitious water [50]. These two species are examples of supramolecular isomers (SI) being supramolecular variants of the basic building block $Cd[S_2CN(iPr)CH_2CH_2OH]_2$. SI originally referred to the phenomenon whereby distinct supramolecular arrangements are constructed from the same building blocks [53]. While this definition allowed for the presence of additional species such as solvent, a more recent definition refers to "genuine SI" where the molecular formula of each isomer is identical [54]; for a discussion on SI terminology see [55]. It should be noted that the terms polymorphism/pseudo polymorphism for the above species are excluded as the nature of the Cd–S bonding is quite distinct in the two structures. Several factors are known to influence the formation of SI with the most significant being solvent [56-61] and temperature [62-66] but other factors such as guest molecules [67], concentration of reagents [68, 69], conformation of molecules [70], molar ratio of reactants [71], and pH of reaction [72, 73] are also known to lead to SI.

The transformation of $[\{Cd[S_2CN(iPr)CH_2CH_2OH]_2\}_3 \cdot MeCN]_\infty$ to $\{Cd[S_2CN(iPr)CH_2CH_2OH]_2\}_2 \cdot 2H_2O \cdot 2MeCN$ mentioned above is an example of solvent induced SI [56-61]. Given the great interest in SI, including recent studies of SI in dithiocarbamates [74-76], it was thought of interest to explore the influence of other solvent systems upon SI in $Cd[S_2CN(iPr)CH_2CH_2OH]_2$. With ethanol as the solvent two new SI, polymeric $[\{Cd[S_2CN(iPr)CH_2CH_2OH]_2\} \cdot EtOH]_\infty$ (**1**) and binuclear $\{Cd[S_2CN(iPr)CH_2CH_2OH]_2\}_2 \cdot 2EtOH$ (**2**), were characterized; their interconversion has also been investigated along with their relationships with the original $[\{Cd[S_2CN(iPr)CH_2CH_2OH]_2\}_3 \cdot MeCN]_\infty$ and $\{Cd[S_2CN(iPr)CH_2CH_2OH]_2\}_2 \cdot 2H_2O \cdot 2MeCN$ SI. From other solvent systems/crystallization conditions a co-crystal (**3**) and a co-crystal salt (**4**), each containing binuclear $\{Cd[S_2CN(iPr)CH_2CH_2OH]_2\}_2$, and a salt (**5**), with $\{Cd[S_2CN(iPr)CH_2CH_2OH]_3\}^-$, were also studied crystallographically. The results of this investigation are reported herein.

Experimental

Instrumentation

All chemicals and reagents were used as received without purification: *N*-isopropyl ethanol amine (70% purity; Aldrich), carbon disulfide (99.9% purity; Merck), sodium hydroxide (≥99.0% purity; Merck), $CdCl_2$ (99.0% purity; Across Organic), $Cd(acetate)_2.2H_2O$ (Fluka), d^6-DMSO (MagniSolv™, Merck), and Emsure® ethanol, acetone, chloroform, hydrochloric acid (37%), and acetonitrile (Merck). Acetonitrile and ethanol used in the solvent mediated transformation experiments were dried over molecu-

lar sieve 3 Å (Merck). For the gel experiments, sodium silicate hexahydrate (99.0% purity; R&M Chemicals) was employed.

Melting points were determined on a Krüss KSP1N melting point meter. Elemental analyses were performed on a Perkin Elmer PE 2400 CHN Elemental Analyser. ^{1}H and $^{13}C\{^{1}H\}$ NMR spectra were recorded in d^6-DMSO solution on a Bruker Avance 400 MHz NMR spectrometer with chemical shifts relative to tetramethylsilane as the internal reference; abbreviations for NMR assignments: *s*, singlet; *d*, doublet; *t*, triplet; *sept*, septet; *m*, multiplet; *dq*, doublet of quartets. The optical absorption spectra were measured in the range 190-1100 nm on an Agilent Cary 60 UV-Vis spectrophotometer. IR spectra were measured on a Perkin Elmer Spectrum 400 FT Mid-IR/Far-IR spectrophotometer from 4000 to 400 cm^{-1}. Thermogravimetric analyses were performed on a Perkin- Elmer TGA 4000 Thermogravimetric Analyzer in the range of 30 − 900 °C at a rate of 10 °C/min.

Synthesis and crystal growth

All reactions were carried out under ambient conditions. The sodium salt of $^{-}S_2CN(iPr)CH_2CH_2OH$ was prepared by reacting NaOH, *N*-isopropyl ethanol amine and CS_2 as detailed earlier [50]. To prepare the $Cd[S_2CN(iPr)CH_2CH_2OH]_2$ precursor, $Na[S_2CN(iPr)CH_2CH_2OH]$ (5.000 g, 0.0248 mol) and $CdCl_2$ (2.273 g, 0.0124 mol) were separately dissolved in water (50 ml). The $CdCl_2$ solution was added slowly into the solution containing the dithiocarbamate anion with stirring. A milky white precipitate formed immediately. This was extracted into chloroform (100 ml), a process repeated several times. The chloroform extract was filtered and dried on a hotplate at 80 ºC overnight (yield (based on Cd): 4.460 g, 76.7%). The compound exhibited the same spectroscopic features as reported earlier [50]. This material was used for the generation of each of **1**–**5**.

Compounds **1** and **2** were obtained by crystallization of the $Cd[S_2CN(iPr)CH_2CH_2OH]_2$ precursor in Emsure® ethanol with **1** being the first crystals formed. With time **1** transformed to **2** as detailed below in the Results and Discussion.

To obtain a sufficient quantity of **1** for physiochemical characterization $Cd[S_2CN(iPr)CH_2CH_2OH]_2$ (0.5 g) was dissolved in Emsure® ethanol (50 ml). Needles of **1**, with composition $[\{Cd[S_2CN(iPr)CH_2CH_2OH]_2\}\cdot EtOH]_\infty$ (see later), were harvested after 3 h (yield (based on Cd): 0.3894 g, 77.9%); M.pt: 152.5-156.1 ºC. Elemental analysis: C, 32.43; H, 5.83; N, 5.11. $C_{14}H_{30}CdN_2O_3S_4$ requires: C, 32.65; H, 5.87; N, 5.44. IR (cm^{-1}): 1446 m *ν*(C–N), 1162 m, 964 m *ν*(C–S). ^{1}H NMR $\{d^6$-DMSO$\}$: δ 5.21 (*sept*, CH, 2H, 6.67 Hz), 4.81 (*t*, $CH_2CH_2O\underline{H}$, 2H, 5.52 Hz), 4.35 (*t*, $CH_3CH_2O\underline{H}$, 1H, 5.08 Hz), 3.60-3.80 (*m*, NCH_2CH_2O, 8H), 3.44 (*dq*, $CH_3C\underline{H}_2OH$, 2H, J_q = 6.98 Hz, J_d = 5.10 Hz), 1.17 (*d*, $CHC\underline{H}_3$, 12H, 6.72 Hz), 1.06 (*t*, $C\underline{H}_3CH_2OH$, 3H, 7.00 Hz) ppm. ^{13}C $\{^{1}H\}$ $\{d^6$-DMSO$\}$: δ 205.12 (CS_2), 58.09 (OCH_2), 56.46 (NCH_2), 55.92 ($CH_3\underline{C}H_2OH$), 50.33

(CH), 19.76 (CH_3), 18.45 ($\underline{C}H_3CH_2OH$) ppm. UV/vis (EtOH:MeCN 1/1 *v*/*v*; 10 μM): λ_{max} = 261 nm (ε = 28450 cm^{-1} M^{-1}); 283 (17830); 338 (199).

Under the same crystallization conditions, blocks of **2** (yield (based on Cd): 0.3392 g, 67.8%) were harvested after three days with composition $\{Cd[S_2CN(iPr)CH_2CH_2OH]_2\}_2 \cdot 2EtOH$; M.pt: 149.0-149.5 ºC. Elemental analysis: C, 32.30; H, 5.74; N, 5.45. $C_{28}H_{60}Cd_2N_4O_6S_8$ requires: C, 32.65; H, 5.87; N, 5.44. IR (cm^{-1}): 1451 m *ν*(C–N), 1160 m, 969 m *ν*(C–S). ^{1}H NMR {d^6-DMSO}: δ 5.21 (*sept*, CH, 2H, 6.66Hz), 4.81 (*t*, $CH_2CH_2O\underline{H}$, 2H, 5.52 Hz), 4.35 (*t*, $CH_3CH_2O\underline{H}$, 1H, 5.08 Hz), 3.60-3.80 (*m*, NCH_2CH_2O, 8H), 3.44 (*dq*, $CH_3C\underline{H}_2OH$, 2H, J_q = 6.69 Hz, J_d = 5.08 Hz), 1.17 (*d*, $CHC\underline{H}_3$, 12H, 6.72 Hz), 1.06 (*t*, $C\underline{H}_3CH_2OH$, 3H, 7.00 Hz) ppm. ^{13}C {^{1}H} {d^6-DMSO}: δ 205.11 (CS_2), 58.09 (OCH_2), 56.46 (NCH_2), 55.92 ($CH_3\underline{C}H_2OH$), 50.32 (CH), 19.76 (CH_3), 18.45 ($\underline{C}H_3CH_2OH$) ppm. UV/vis (EtOH:MeCN 1/1 *v*/*v*; 10 μM): λ_{max} = 261 nm (30200 cm^{-1} M^{-1}); 283 (18860); 340 (ε = 213).

Crystals of **3**, characterised crystallographically as a 1:2 co-crystal comprising $\{Cd[S_2CN(iPr)CH_2CH_2OH]_2\}_2$:2[3-(propan-2-yl)-1,3-oxazolidine-2-thione], were obtained by slow evaporation of a portion of one the chloroform solutions (100 ml) used for the extraction of the $Cd[S_2CN(iPr)CH_2CH_2OH)]_2$ precursor.

Crystals of **4** were obtained by dissolving $Cd[S_2CN(iPr)CH_2CH_2OH]_2$ (0.5 g) in acetone (100 ml). The solution was stirred at 50 ºC for 1 h. After filtration the solution was kept under ambient conditions which yielded a small number of crystals after 2 days. These were formulated on the basis of X-ray crystallography as a salt co-crystal $[iPrNH_2(CH_2CH_2OH)]_2[SO_4]$-$\{Cd[S_2CN(iPr)CH_2CH_2OH]_2\}_2$.

Crystals of **5** were isolated from a crystallization experiment in a sodium silicate gel. $Cd(acetate)_2.2H_2O$ (0.5683 g, 2.13 mmol) was dissolved in a sodium silicate gel solution (35 ml of 1.03 g ml^{-1}). The pH of the solution was adjusted to 6.0-7.0 by 5M hydrochloric acid. The gel solution was transferred to an 80 ml test tube and allowed to stand overnight. $Na[S_2CN(iPr)CH_2CH_2OH]$ (0.8584 g, 4.26 mmol) dissolved in water (35 ml) was carefully layered on top of the gel. A small number of crystals formed after 1 month. These were formulated as the salt $[iPrNH_2(CH_2CH_2OH)]\{Cd[S_2CN(iPr)CH_2CH_2OH]_3\}$ by X-ray crystallography.

As only a matter of a few crystals were obtained for each of **3**–**5** there was insufficient sample for additional physiochemical characterization.

Crystal structure determination

Single crystal X-ray diffraction data for colourless **1** (0.06 x 0.08 x 0.12 mm; cut from a needle), **2** (0.15 x 0.20 x 0.25 mm) and **3** (0.13 x 0.20 x 0.20 mm) were measured on a Bruker SMART APEX CCD diffractometer. Data for colourless **4** (0.05 x 0.10 x 0.20 mm) and yellow **5** (0.20 x 0.25 x 0.30 mm) were measured on an Agilent Technologies SuperNova Dual diffractometer fitted with an Atlas (Mo)

detector. Data collections were measured at 100 K and employed Mo Kα radiation (λ = 0.71073 Å) to θ_{max} of 27.5°. A multi-scan absorption correction was applied in each case [77, 78]. The structures were solved by direct methods (SHELXS97 [79]) and refined (anisotropic displacement parameters (ADP), C-bound H atoms in the riding model approximation and a weighting scheme of the form $w = 1/[\sigma^2(F_o^2) + aP^2 + bP]$ where $P = (F_o^2 + 2F_c^2)/3)$ with SHELXL2014 on F^2 [80]. The O-bound H atoms were located from difference maps and generally included in the refinement with O–H = 0.84±0.01 Å. When present N-bound H atoms were refined with N–H = 0.91±0.01 Å. Crystal data and refinement details are collected in Table 1. Several of the refinements were non-trivial. In **1**, the methylene group of the ethanol molecule was statistically disordered. The ADP for both components of the disorder were constrained to be equal and along with the terminal methyl group to be approximately isotropic. Further, some soft distance restraints were employed for this molecule i.e. C–O, C–C, and O…C(methyl) were refined with 1.47±0.01, 1.50±0.01 Å, and 2.45±0.01 Å, respectively. All acidic protons were found to be disordered over two positions in locations consistent with hydrogen bonding to O atoms. In the final refinement O–H bond lengths were fixed in their as located positions i.e. 0.83-0.85 Å. Three reflections, i.e. (0 0 2), (-1 0 10) and (-3 0 30), were omitted from the final cycles of refinement owing to poor agreement, i.e. the "error/esd" calculated by SHELXL2014 was greater than 10. Finally, the maximum and minimum residual electron density peaks, Table 1, were located 0.75 and 0.72 e Å^{-3} from the Cd1 and Cd2 atoms, respectively. In **2**, both the ethanol- and O1-hydroxyethyl-OH groups were statistically disordered; ADP for the chemically equivalent disordered components were constrained to be equal. For the ethanol molecule both O atoms were connected to the same H atom. For the O1-hydroxyl group only one position was found for the hydroxyl-H atom (assigned full weight) based on anticipated O–H…O hydrogen bonding. Four reflections were omitted from the final refinement of **3**, i.e. (-6 -5 1), (12 -1 1), (-6 -5 14) and (-2 6 1), again owing to poor agreement. For **4**, the O2-hydroxyethyl residue, with the exception of the hydroxyl-H atom, was disordered over two positions in a ratio 0.851(2):0.149(2). The ADP of matching pairs of atoms were constrained to be equal and nearly isotropic. Further, chemically equivalent bond lengths were constrained to be nearly equal. The residual electron density peaks, Table 1, were located 1.46 and 0.67 e Å^{-3} from the S4 and S5 atoms, respectively. Two low angle reflections were omitted from the final refinement of **5**, i.e. (0 2 0) and (-1 0 1), as these were affected by the beam-stop and exhibited poor agreement. The displacement ellipsoid diagrams were drawn with ORTEP-3 for Windows [81] at the 50% probability level and other crystallographic diagrams were drawn with DIAMOND [82] and QMol [83].

Table 1. Crystallographic data and refinement details for **1**-**5**.[1]

Parameter	**1**	**2**	**3**	**4**	**5**
Formula	$C_{12}H_{24}CdN_2O_2S_4$	$C_{24}H_{48}Cd_2N_4O_4S_8$	$C_{24}H_{48}Cd_2N_4O_4S_8$	$C_{24}H_{48}Cd_2N_4O_4S_8$	$C_{18}H_{36}CdN_3O_3S_6$
	CH_3CH_2OH	$2CH_3CH_2OH$	$2(C_6H_{11}NOS)$	$4(C_5H_{14}NO)$, $2(SO_4)$	$C_5H_{14}NO$
Formula weight	515.04	1030.10	1228.50	1546.75	751.43
Crystal system	monoclinic	triclinic	triclinic	monoclinic	monoclinic
Space group	*P*2/*c*	$P\bar{1}$	$P\bar{1}$	*C*2/*c*	$P2_1/n$
a/Å	10.2768(2)	9.2310(18)	10.419(2)	29.3471(6)	10.6261(2)
b/Å	7.6850(2)	9.2847(19)	11.120(2)	11.2512(2)	17.7820(4)
c/Å	27.9859(6)	13.671(3)	13.119(3)	21.9269(4)	17.8128(4)
α/º	90	83.15(3)	106.64(3)	90	90
β/º	90.839(1)	82.22(3)	102.07(3)	101.959(2)	91.274(2)
γ/º	90	71.73(3)	107.68(3)	90	90
V/Å^3	2210.01(9)	1098.7(4)	1312.5(5)	7082.9(2)	3364.96(12)
Z	4	1	1	4	4
Dc/g cm^{-3}	1.548	1.557	1.554	1.450	1.483
μ(MoKα)/mm^{-1}	1.380	1.388	1.253	0.956	1.055
Reflections collected	20074	13965	16418	28643	22504

Independent reflections	5069	4962	5907	8005	7715
Reflections with $I \geq 2\sigma(I)$	4033	4526	5085	7010	6382
R (observed data)	0.037	0.023	0.025	0.025	0.027
a; b in weighting scheme	0.018; 6.753	0.026; 0.169	0.034; 0	0.029; 7.020	0.017; 0.735
R_w (all data)	0.076	0.054	0.064	0.062	0.057
Largest diff. peak and hole e Å^{-3}	1.46; -1.40	0.40; -0.50	0.69; -0.48	1.41; -0.40	0.42; -0.42

[1] Supplementary Material: Crystallographic data (excluding structure factors) for the structures reported in this paper have been deposited with the Cambridge Crystallographic Data Centre as supplementary publications no. CCDC-1405102 to 1405106. Copies of available material can be obtained free of charge, on application to CCDC, 12 Union Road, Cambridge CB2 1EZ, UK, (fax: +44-(0)1223-336033 or e-mail: deposit@ccdc.cam.ac.uk). The list of Fo/Fc-data is available from the author up to one year after the publication has appeared.

Powder X-ray Diffraction

Powder X-ray diffraction (PXRD) data were recorded with a PANalytical Empyrean XRD system with Cu Kα1 radiation (λ = 1.54056 Å) in the 2θ range of 5 to 40° with a step size of 0.026°. The comparison between experimental and calculated (from CIFs) PXRD patterns was performed with X'Pert HighScore Plus [84].

Results and Discussion

Synthesis and solution characterization

As reported earlier [50], the metathetical reaction between $CdCl_2$ and 2 molar equivalents of $Na[S_2CN(iPr)CH_2CH_2OH)]$ yielded the anticipated cadmium bis(dithiocarbamate) compound (based on ^1H and ^{13}C NMR), $Cd[S_2CN(iPr)CH_2CH_2OH]_2$; this was isolated as an analytically pure powder. Recrystallization from Emsure® ethanol solution resulted in X-ray quality acicular crystals of **1** within 3 h, Fig. 1a. After only an additional hour of crystallization, blocks of **2** started to appear with the needles of **1** being subsumed, Fig. 1b, with the transformation nearly complete after 6 h, Fig. 1c. After 3 days there was no evidence for acicular crystals, Fig. 1d. Such transformation and change in morphology indicates disassembly of the original crystals and reassembly into the new form [85].

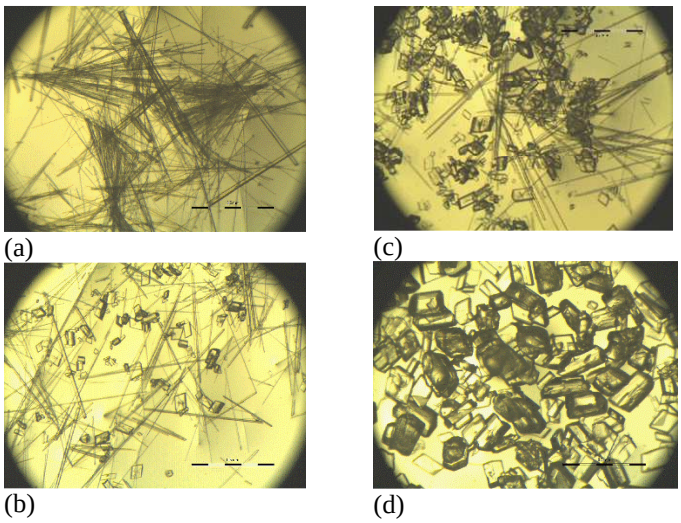

Fig. 1. Formation of crystals of needles of **1** and blocks of **2** in Emsure® ethanol solution after: (a) 3 h, (b) 4 h, (c) 5 h and (d) 3 days.

The IR spectra recorded on freshly isolated crystals presented a very similar pattern of absorptions with minor differences in wavenumbers. ^1H NMR spectroscopy conducted on analytically pure crystals of **1** and **2** were indistinguishable in terms of chemical shifts, integration and multiplicity indicating they have the same chemical composition confirmed by X-ray crystallography (see below). Remarkably, both hydroxyethyl- and ethanol-OH protons

appeared as well defined triplets. Similarly, the ^{13}C NMR were indistinguishable as were the UV/vis spectra.

The crystal and molecular structures of **1** and **2** were determined showing the compositions of the needles and blocks to be polymeric $[\{Cd[S_2CN(iPr)CH_2CH_2OH]_2\}\cdot EtOH]_\infty$ (**1**) and binuclear $\{Cd[S_2CN(iPr)CH_2CH_2OH]_2\}_2\cdot 2EtOH$ (**2**), respectively i.e. to be (genuine) supramolecular isomers in the sense that the empirical formula of each of **1** and **2** is identical. The similarity of the solution characterization (^{1}H and ^{13}C{^{1}H} NMR and UV/vis) for both species proves the observed SI to be a solid-state phenomenon.

Single crystal X-ray crystallography

The crystallographic asymmetric unit of $[\{Cd[S_2CN(iPr)CH_2CH_2OH]_2\}\cdot EtOH]_\infty$ (**1**), comprises two independent Cd atoms, each located on a 2-fold axis, two dithiocarbamate ligands and an ethanol molecule, Fig. 2a. Both dithiocarbamate ligands coordinate in a $\mu_2\kappa^2$-tridentate mode, simultaneously chelating one Cd atom and bridging another. This results in octahedrally coordinated Cd atoms and the formation of a 1-D coordination polymer comprising alternating Cd1 and Cd2 atoms aligned along the *b*-axis, Fig. 2b. The Cd–S bond lengths, Table 2, span a relatively narrow range with the range for the Cd1 atom, i.e. 2.6331(8) to 2.7412(9) Å, being wider than for Cd2, i.e. 2.6556(9) to 2.7122(9) Å. Distortions from the ideal octahedral geometry can be related to the restricted bite angles of the dithiocarbamate ligands, i.e. 67-68º. The trans-S–Cd–S angles lie in a narrow range i.e. 167-168º.

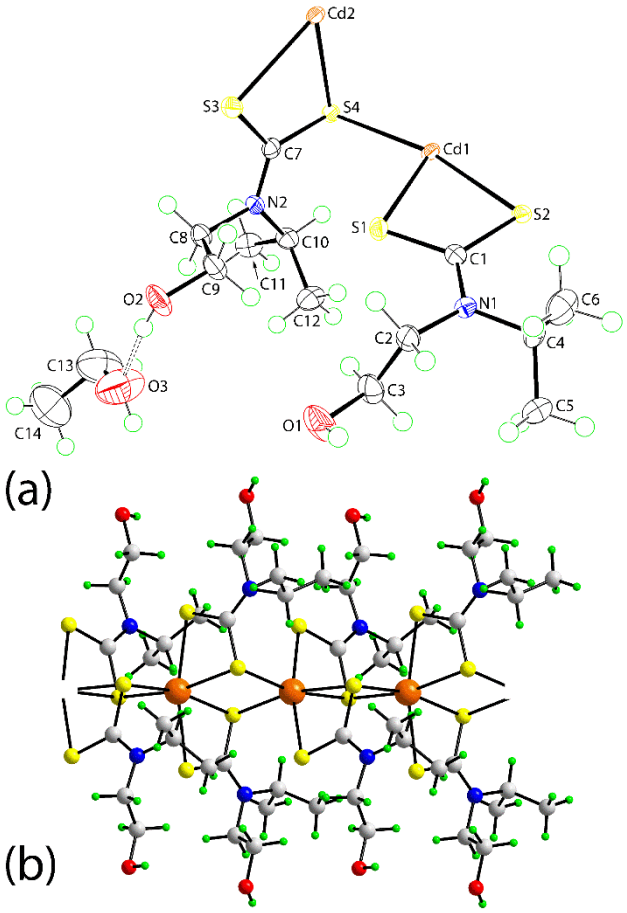

Fig. 2. (a) The asymmetric unit for **1** showing atom labelling scheme; only one orientation of the disordered components is shown, and (b) the 1-D coordination polymer with ethanol molecules omitted. In all images only one orientation of the acidic-H atoms is shown.

Table 2. Summary of key geometric parameters (Å, º) for **1** and **2**.[1]

Compound	Parameter
1	
Cd1–S1, S2, S4	2.6331(8), 2.7412(9), 2.6890(9)
Cd2–S3, S4, S2^{i}	2.6556(9), 2.7122(9), 2.6811(9)
2	
Cd–S1, S2	2.5462(8), 2.6152(9)
Cd–S3, S4, S4^{ii}	2.5289(8), 2.8067(8), 2.6090(9)

[1] Symmetry operations, *i*: *x*, -1+*y*, *z*; *ii*: 1-*x*, 1-*y*, -*z*.

In the crystals of **1** supramolecular chains are formed by O–H…O hydrogen bonding involving the hydroxylethyl- and ethanol-hydroxyl groups with one orientation of these interactions illustrated in Fig. 3a; the geometric characteristics of the intermolecular interactions operating in the crystal structures of **1** and **2** are listed in Table 3. As the 1-D coordination polymers are connected by hydrogen bonding

along both the *a*- and *c*-axes so that a 3-D architecture arises, Fig. 3b.

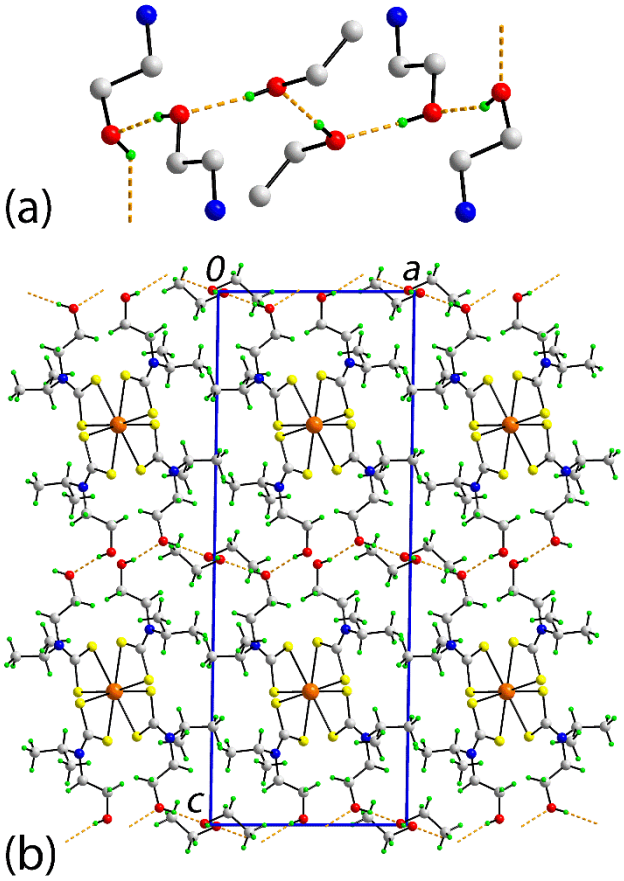

Fig. 3. (a) A supramolecular chain in **1** mediated by O–H…O hydrogen bonding (orange dashed lines) with most atoms omitted, and (b) a view of the unit cell contents in projection down the *b*-axis. In all images only one orientation of the acidic-H atoms is shown.

Table 3. Summary of intermolecular interactions (A–H···B; Å, º) operating in the crystal structures of **1** and **2**.

A	H	B	H···B	A···B	A–H···B	symmetry operation
1						
O1	H1o	O2	1.93	2.716(4)	157	1-*x*, 1-*y*, 1-*z*
O1	H1o'	O1	2.00	2.717(4)	142	1-*x*, 1-*y*, 1-*z*
O2	H2o'	O1	1.89	2.716(4)	170	1-*x*, 1-*y*, 1-*z*
O2	H2o	O3	1.89	2.718(5)	172	*x*, *y*, *z*
O3	H3o	O3	1.91	2.744(5)	174	-*x*, 1-*y*, 1-*z*
O3'	H3o'	O2	1.90	2.718(5)	163	x, y, z
2						
O1	H1o	O3	1.94(2)	2.739(6)	168(3)	1-*x*, 1-*y*, 1-*z*
O2	H2o	O1	1.939(14)	2.769(6)	174(2)	*x*, 1+*y*, -1+*z*
O2	H2o	O1'	1.975(17)	2.785(6)	164(3)	*x*, 1+*y*, -1+*z*
O3	H3o	O2	1.96(5)	2.787(4)	167(5)	-1+*x*, *y*, 1+*z*
O3'	H3o'	O2	1.88(4)	2.713(3)	170(5)	1-*x*, 1-*y*, -*z*

As illustrated in Fig. 4a, the asymmetric unit of **2** comprises half a molecule of $\{Cd[S_2CN(iPr)CH_2CH_2OH]_2\}_2$ and an ethanol molecule. The full molecule of $\{Cd[S_2CN(iPr)CH_2CH_2OH]_2\}_2$ is generated by the application of a centre of inversion, Fig. 4b, i.e. being the common structural motif for molecules of the general formula $\{Cd[S_2CNRR']_2\}_2$ [31-49]. In this structure the S1- and S3 dithiocarbamate ligands are κ^2-chelating and $\mu_2\kappa^2$-tridentate, respectively, resulting in five coordinate geometries based on square pyramidal geometries as seen in the τ value of 0.08 which compares to τ values of 0.00 and 1.00 for ideal square pyramidal and trigonal bipyramidal geometries, respectively [86]. In this description the bridging S4 atom occupies the axial position.

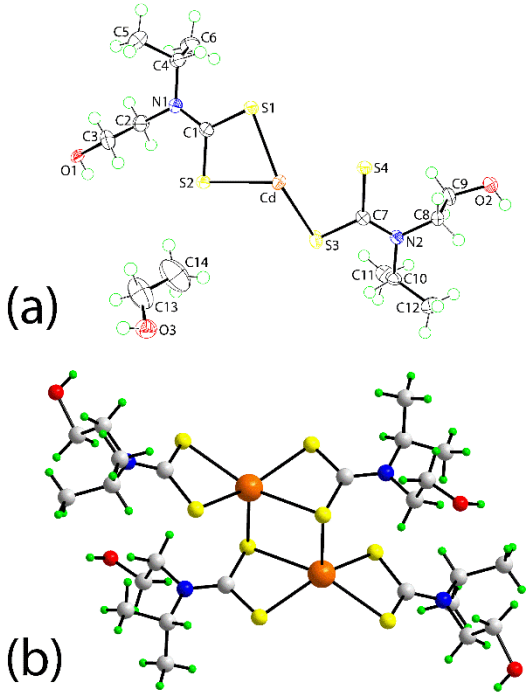

Fig. 4. (a) The symmetric unit for **2** showing atom labelling scheme, and (b) a view of the centrosymmetric binuclear molecule with ethanol molecules omitted. In all images only one orientation of the disordered components is shown.

The most prominent feature of the molecular packing is the formation of centrosymmetric 12-membered $\{\cdots HO\}_6$ synthons with both hydroxyethyl- and ethanol-hydroxyl groups participating in donor and acceptor O–H···O hydrogen bonds, Fig. 3a and Table 3. The hydrogen bonding leads to the formation of layers parallel to (0 2 1), Fig. 3b; layers stack without specific interactions between them, Fig. 3c.

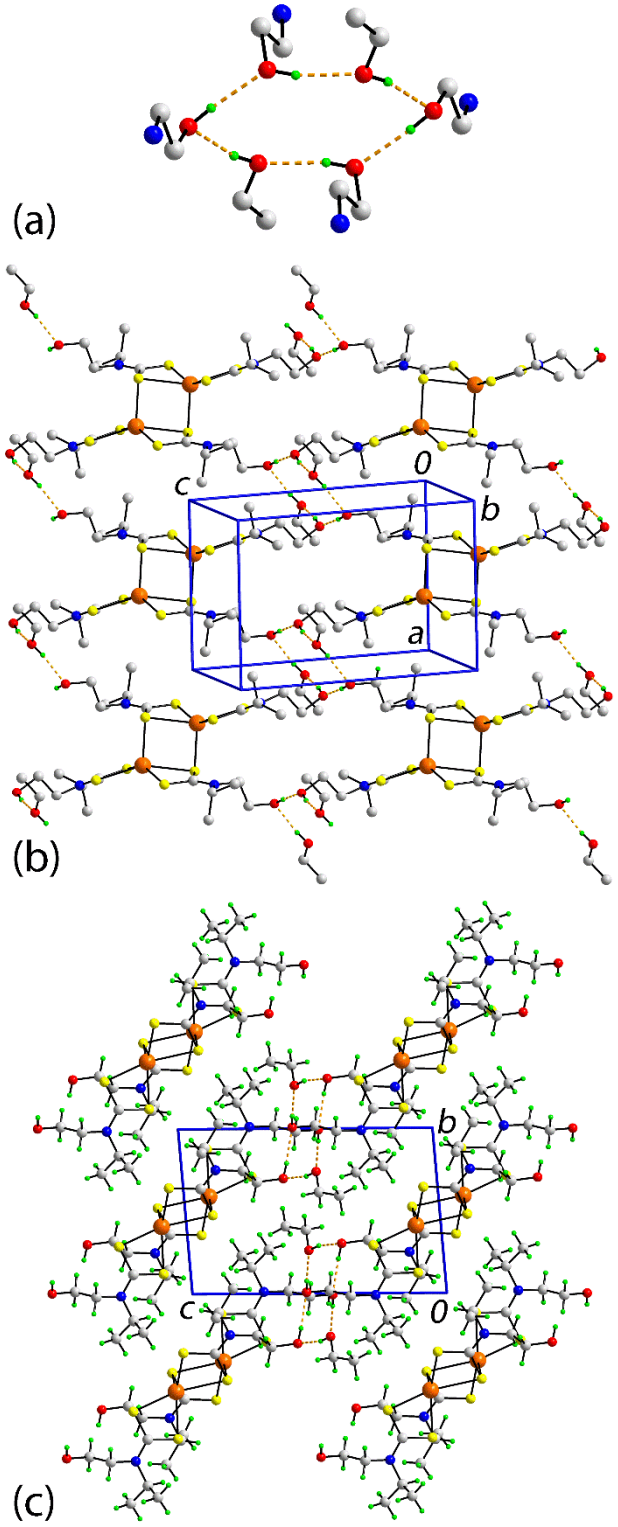

Fig. 5. (a) A supramolecular 12-membered ring in **2** mediated by O–H···O hydrogen bonding (orange dashed lines) with most atoms omitted, (b) a view of the supramolecular layer parallel to (0 2 1), and (c) a view of the unit cell contents shown in projection down the *a*-axis highlighting the stacking of layers. In all images only one orientation of the disordered components is shown.

Powder X-ray diffraction (PXRD)

PXRD experiments were performed on freshly isolated **1** and **2** and compared with the simulated patterns calculated from the single crystal (SCXRD) experiments measured at 100 K. As both pairs of patterns matched, the SCXRD results are representative of the bulk materials, see Fig. S1 of the Supplementary Material. The stability of **1** and **2** with respect to loss of ethanol was also investigated using PXRD. Thus, time-dependent PXRD were measured on freshly harvested crystals and subsequently at 2, 6, 12, and 24 h; the experimental traces are given in Supplementary Material Fig. S2. For both **1** and **2** changes were apparent before 2 h indicating loss of the original crystal structure. The patterns obtained for **1** and **2** after 24 h were distinct from each other and different from the original material used for recrystallization, i.e. $Cd[S_2CN(iPr)CH_2CH_2OH]_2$; see Supplementary Material Fig. S2c.

Thermal degradation

The TGA traces for **1** and **2** are shown in Supplementary Material Fig. S3. Each decomposes in two well-defined steps to yield CdS. For **1** the desolvation of lattice ethanol occurred in the first step between 57 and 120 ºC with a weight loss of 7.1% *cf*. calc'd. 8.9%. The second step between 120 and 338 ºC left a residue of 27.2 % *cf*. calc'd. 28.0% corresponding to CdS; cadmium dithiocarbamates [2, 50] and the nitrogen adducts [87, 88] are known to be excellent synthetic precursors for the deposition of CdS nanoparticles. The corresponding temperature ranges for **2** are 65 to 149 ºC (obs., calc'd. weight loss: 8.0, 8.9%) and 149 to 356 ºC (29.6, 28.0%). The stability of **1** and **2** was also monitored by time dependent TGA where scans were performed on a fresh sample and then at 2, 6, 12, and 24 h; see Supplementary Material Fig. S3. By 6 h, practically all of the lattice ethanol had evaporated, a process that resulted in a change in crystal structure as indicated by the time dependent PXRD study (see above).

Relationship between SI formed from $Cd[S_2CN(iPr)CH_2CH_2OH]_2$

With the characterization of **1** and **2**, there are now three distinct SI derived from the basic building block, $Cd[S_2CN(iPr)CH_2CH_2OH]_2$, with the third being the previously reported $[\{Cd[S_2CN(iPr)CH_2CH_2OH]_2\}_3\cdot MeCN]_\infty$ (**6**) [50]; the SI in $\{Cd[S_2CN(iPr)CH_2CH_2OH]_2\}_2\cdot 2H_2O\cdot 2MeCN$ (**7**) [50] matches that of **2**. Fig. 6 shows simplified representations of the three SI, i.e. the dimer in **2** (and **7**), and the linear coordination polymers in each of **1** and **6**. The relationships between the SI are quite straight forward. In **2**, only one dithiocarbamate ligand forms Cd–S bridges so that a dimeric aggregate is formed. By contrast, in each of **1** and **6**, both dithiocarbamates form Cd–S bridges leading to linear coordination polymers. The primary difference between **1** and **6** rests with the relative orientation of the dithiocarba-

mate ligands. In **1**, with crystallographically imposed 2-fold symmetry, the dithiocarbamate ligands are oriented in the same direction whereas in **6**, with neighbouring cadmium atoms related by centres of inversion, alternate dithiocarbamate ligands are oriented in opposite directions.

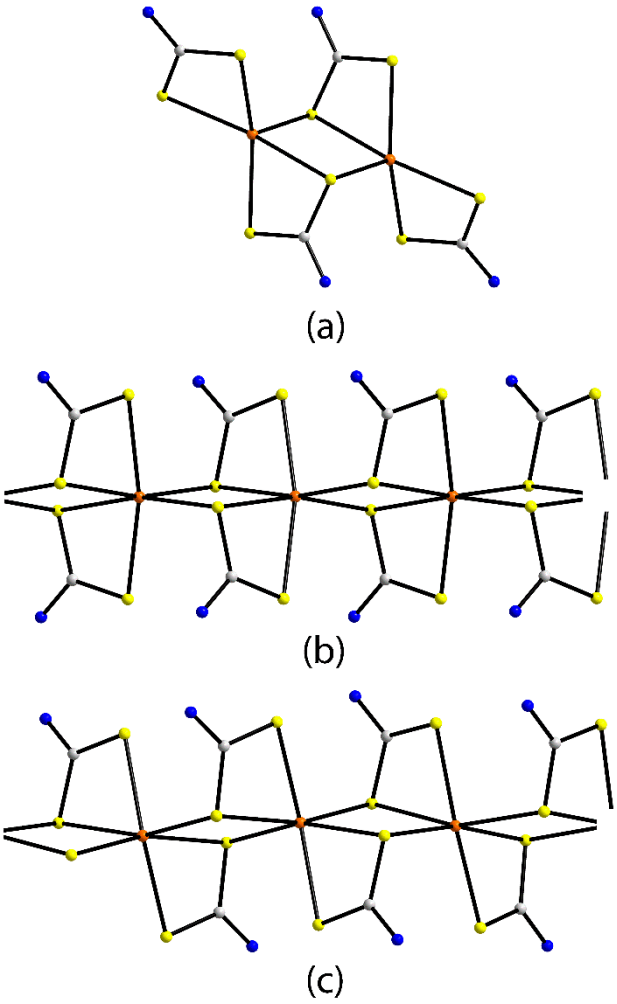

Fig. 6. Schematic images of the three SI derived from $Cd[S_2CN(iPr)CH_2CH_2OH]_2$: (a) dimeric **2**, and linear coordination polymers (b) **1** and (c) **6**. Alkyl substituents have been removed for clarity.

Conversion between SI

Conversion between coordination polymers, including SI, in the solid state has been reviewed [89]. Examples exist whereby reversible single crystal single crystal transformations mediated by solvent guests [90, 91], recrystallization [92] and microwave irradiation/rehydration [93, 94]. Given the similarity in the SI derived from $Cd[S_2CN(iPr)CH_2CH_2OH]_2$, it was thought of interest to investigate whether solvent mediated interconversion between them was possible.

The in situ conversion of $[\{Cd[S_2CN(iPr)CH_2CH_2OH]_2\}\cdot EtOH]_\infty$ (**1**) to $\{Cd[S_2CN(iPr)CH_2CH_2OH]_2\}_2.2EtOH$ (**2**) indicates that the kinetic SI, **1**, transforms to the thermodynamic form, **2**,

with time. In the previous study of $[\{Cd[S_2CN(iPr)CH_2CH_2OH]_2\}_3\cdot MeCN]_\infty$ (**6**) and $\{Cd[S_2CN(iPr)CH_2CH_2OH]_2\}_2\cdot 2H_2O\cdot 2MeCN$ (**7**) it was concluded that adventitious water mediated the in situ transformation of **6** to **7** [50]. In order to investigate if was possible to interconvert the SI, additional experiments were conducted. In these experiments freshly isolated samples (0.1 g) of **1**, **2**, **6** and **7** were taken up in dry (3 Å molecular sieves) and laboratory grade Emsure® MeCN or EtOH, covered with parafilm (with a few holes), and allowed to crystallise over seven days. The resultant crystals were analysed by PXRD (see Supplementary Material Fig. S4). Fig. 7 summarizes the observed conversions between the SI achieved under these conditions.

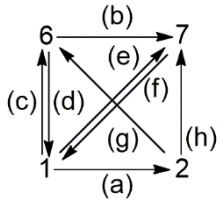

Fig. 7. Solvent mediated interconversion between $[\{Cd[S_2CN(iPr)CH_2CH_2OH]_2\}\cdot EtOH]_\infty$ (**1**), $\{Cd[S_2CN(iPr)CH_2CH_2OH]_2\}_2.2EtOH$ (**2**), $[\{Cd[S_2CN(iPr)CH_2CH_2OH]_2\}_3\cdot MeCN]_\infty$ (**6**), and $\{Cd[S_2CN(iPr)CH_2CH_2OH]_2\}_2\cdot 2MeCN\cdot 2H_2O$ (**7**). (a) in dry or lab. grade EtOH under ambient conditions, (b) dry MeCN and adventitious water, (c) dry MeCN and stored in a desiccator, (d) dry EtOH in a desiccator, (e) dry or lab. grade MeCN under ambient conditions, (f) lab. EtOH under ambient conditions, (g) dry MeCN in a desiccator, and (h) dry or lab. grade MeCN under ambient conditions.

A reversible transformations between polymeric **1** and **6** was accomplished by recrystallization from dry acetonitrile and ethanol, respectively. When water was present, adventitious or otherwise, **1** could be converted to dimeric **7** but this was reversible in an excess of dry ethanol presumably as the water released from **7** was associated with the bulk solvent; evidence for a small amount of original **7** was seen in the PXRD for the transformation of **7** to **1** (see Supplementary Material Fig. S4e). Dimeric **2** was mainly (there was also a trace of an unknown species, see Supplementary Material Fig. S4f) transformed to polymeric **6** in an excess of dry acetonitrile but **6** could not be converted back to **2** by simple recrystallization. Similarly **2** was transformed irreversibly to dimeric **7**. A noteworthy observation is that **1**, which is thermodynamically unstable with "genuine SI" **2**, can be maintained in the presence of MeCN. In summary, the above observations are consistent with the overall preferential formation of dimeric **2** and **7**, a result consistent with the literature precedents which overwhelmingly adopt the dimeric motif [31-49].

Complementary crystallization experiments

Given the interesting supramolecular isomerism of and interrelationships between **1**, **2**, **6** and **7**, it was thought of

interest to explore other crystallizing solvents and techniques to investigate whether other supramolecular isomers could be revealed. In all, three additional compounds, namely **3**–**5**, two of which contain binuclear{Cd[S_2CN(iPr)CH_2CH_2OH]$_2$}$_2$ (**3** and **4**) and one with the {Cd[S_2CN(iPr)CH_2CH_2OH]$_3$}$^-$ anion (**5**), were discovered and these are described in turn below.

Compound **3** was isolated from the slow evaporation of a chloroform extract and is formulated as a 1:2 co-crystal, {Cd[S_2CN(iPr)CH_2CH_2OH]$_2$}$_2$:2[3-(propan-2-yl)-1,3-oxazolidine-2-thione], with the asymmetric unit comprising half a molecule of the former and a full molecule of the latter, Fig. 8a. The binuclear molecule, Fig. 8b, is centrosymmetric and to a first approximation exhibits the same features as seen in 2 with the most notable difference being the weakening of the transannular interaction formed by the bridging S2 atom to 3.0448(9) Å, Table 4, cf. the equivalent bond in **2**, Table 2. This has the result that the eight-membered {CdSCS}$_2$ ring lacks the internal Cd_2S_2 square. The reason for this structural difference is not immediately clear but the bridging bond formed by S2 has shortened to 2.5545(11) Å. The oxazolidine molecule is known to be a decomposition/cyclization product derived from the $^-$$S_2$CN(iPr)$CH_2CH_2$OH anion [95], a phenomenon reported for related species [96, 97], and its molecular structure [95] matches closely that observed in **3** as seen the overlay diagram in Fig. 9.

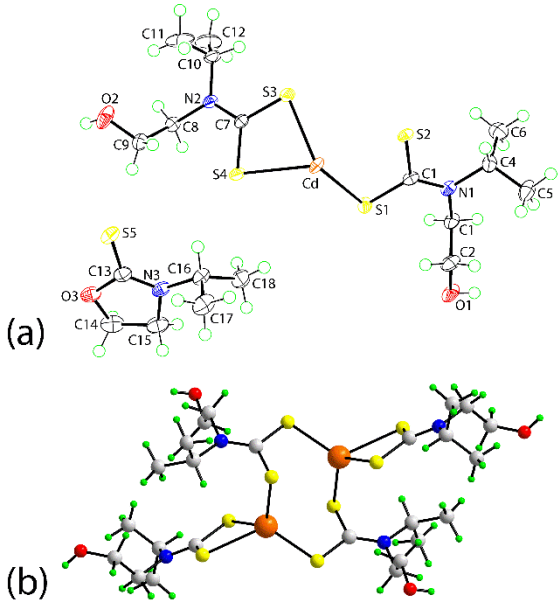

Fig. 8. (a) The asymmetric unit for co-crystal **3** showing atom labelling scheme, and (b) a view of the centrosymmetric binuclear molecule with oxazolidine molecules omitted.

Table 4. Summary of key geometric parameters (Å, º) for **3**-**5**.[1]

Compound	Parameter
3	
Cd–S1, S2, S2^{i}	2.4236(7), 3.0448(9), 2.5545(11)
Cd–S3, S4	2.5109(8), 2.7159(10)
4	
Cd–S1, S2	2.5590(5), 2.5952(5)
Cd–S3, S4, S4^{ii}	2.5619(5), 2.7915(5), 2.5879(5)
5	
Cd–S1, S2	2.6534(6), 2.7040(6)
Cd–S3, S4	2.6787(6), 2.7039(6)
Cd–S5, S6	2.7079(5), 2.7279(5)

[1] Symmetry operations, *i*: -*x*, 1-*y*, 1-*z*; and *ii*: 1-*x*, 2-*y*, 1-*z*

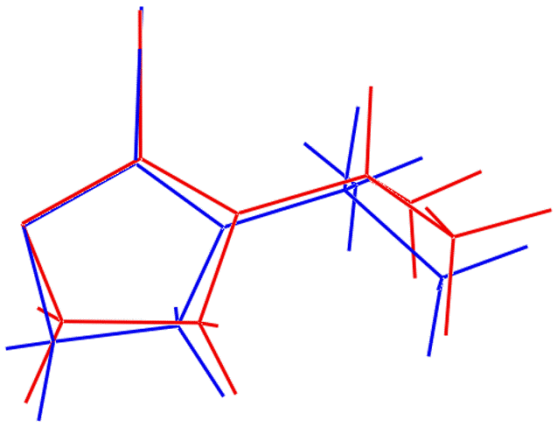

Fig. 9. Overlay diagram of the 3-(propan-2-yl)-1,3-oxazolidine-2-thione molecules in **3** (red image) and in the free form (blue image). The molecules have been overlapped so that the SCO atoms are coincident.

In the molecular packing, hydroxyl-O–H···O(hydroxyl) hydrogen bonds link the binuclear molecules into supramolecular chains aligned along the *a*-axis. Connected to either side of the chain via hydroxyl-O–H···S(oxazolidine) hydrogen bonds are the 3-(propan-2-yl)-1,3-oxazolidine-2-thione molecules, Fig. 10a and Table 5. The chains are connected into a supramolecular layer parallel to (0 1 1) via a strong methyl-C–H…O(hydroxyl) and several C–H…S(dithiocarbamate) interactions; see Fig. 10b.

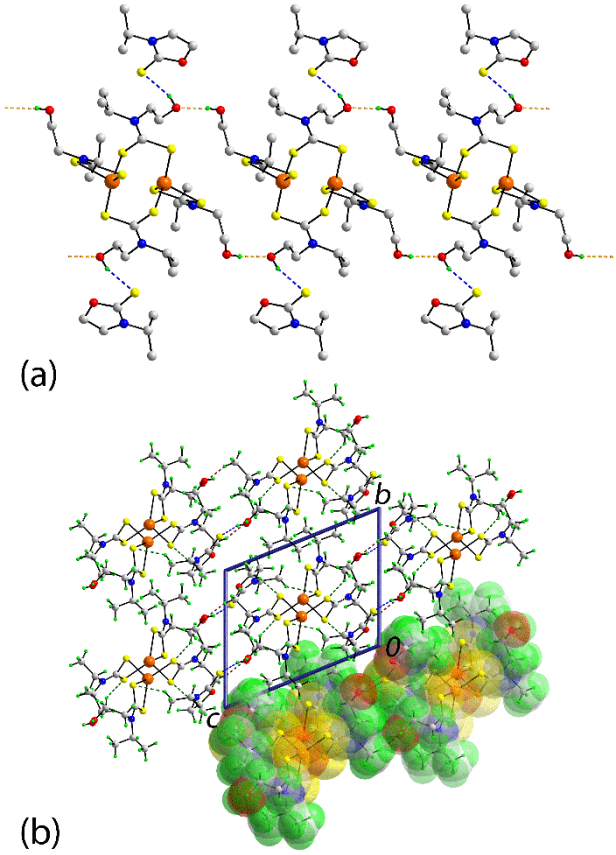

Fig. 10. (a) A supramolecular chain in **3** mediated by O–H···O hydrogen bonding (orange dashed lines) being connected to molecules via O–H···S hydrogen bonds (blue dashed lines) with non-participating H atoms omitted, and (b) a view of the unit cell contents shown in projection down the *a*-axis highlighting the stacking of layers; one layer is shown in space filling mode.

When a sample of $Cd[S_2CN(iPr)CH_2CH_2OH]_2$ was taken in acetone and left to evaporate a small number of crystals formed and these were formulated from X-ray crystallography as the salt co-crystal $[iPrNH_2(CH_2CH_2OH)]_4[SO_4]_2\{Cd[S_2CN(iPr)CH_2CH_2OH]_2\}_2$ (**4**). The asymmetric unit, Fig. 11, comprises half a centrosymmetric $\{Cd[S_2CN(iPr)CH_2CH_2OH]_2\}_2$ molecule, two ammonium $[iPrNH_2(CH_2CH_2OH)]^+$ cations and a sulfate dianion. Presumably the ions are derived from the decomposition and subsequent protonation and oxidation of dithiocarbamate residues, respectively. The neutral species is binuclear and features the same pattern of Cd–S bond lengths as for **2**, Table 4. There are no literature precedents [98] for the structure of the cation (see discussion below).

Table 5. Summary of intermolecular interactions (A–H···B; Å, º) operating in the crystal structures of for **3**-**5**.[1]

A	H	B	H···B	A···B	A–H···B	symmetry operation
3						
O1	H1o	S5	2.56(2)	3.349(2)	158(2)	-1+*x*, *y*, -1+*z*
O2	H2o	O1	1.96(2)	2.781(3)	172(4)	1-*x*, 1-*y*, 1-*z*
C6	H6c	O2	2.19	3.104(3)	155	-1+*x*, *y*, -1+*z*
C9	H9a	S1	2.64	3.536(2)	151	1-*x*, 1-*y*, 1-*z*
C14	H14a	S2	2.77	3.744(3)	169	1-*x*, 1-*y*, 1-*z*
C18	H18b	S4	2.78	3.629(3)	146	1-*x*, 1-*y*, 1-*z*
4						
O1	H1o	O4	2.02(2)	2.850(2)	174(2)	½-*x*, 1½-*y*, 1-*z*
O2	H2o	O5	2.03(2)	2.815(2)	157.7(16)	*x*, *y*, *z*
O3	H3o	O6	1.904(14)	2.7258(18)	167(2)	*x*, *y*, *z*
O4	H4o	O7	1.968(14)	2.7757(19)	164(2)	*x*, *y*, *z*
N3	H1n	O8	1.851(18)	2.727(2)	162.9(17)	*x*, 1-*y*, ½+*z*
N3	H2n	O7	1.982(18)	2.8199(19)	153.6(17)	*x*, *y*, *z*
N4	H3n	O5	1.905(15)	2.804(2)	172.3(19)	*x*, *y*, *z*
N4	H4n	O8	1.865(16)	2.761(2)	168.6(19)	*x*, 1-*y*, ½+*z*
5						
O1	H1o	S3	2.545(13)	3.3189(17)	156(2)	-½+*x*, 1½-*y*, -½+*z*
O2	H2o	S6	2.538(17)	3.3283(16)	160(2)	1+*x*, *y*, *z*
O3	H3o	S5	2.350(13)	3.1475(15)	162(2)	*x*, *y*, *z*
O4	H4o	O2	1.971(19)	2.758(2)	159(2)	*x*, *y*, *z*
N4	H1n	O4	2.38(2)	2.835(3)	111.5(14)	*x*, *y*, *z*
N4	H1n	O4	2.329(18)	2.964(2)	127.4(17)	2-*x*, 1-*y*, 1-*z*
N4	H2n	O1	1.916(13)	2.781(2)	158(2)	1-*x*, 1-*y*, 1-*z*
C9	H9a	O3	2.51	3.423(3)	153	½+*x*, 1½-*y*, -½+*z*

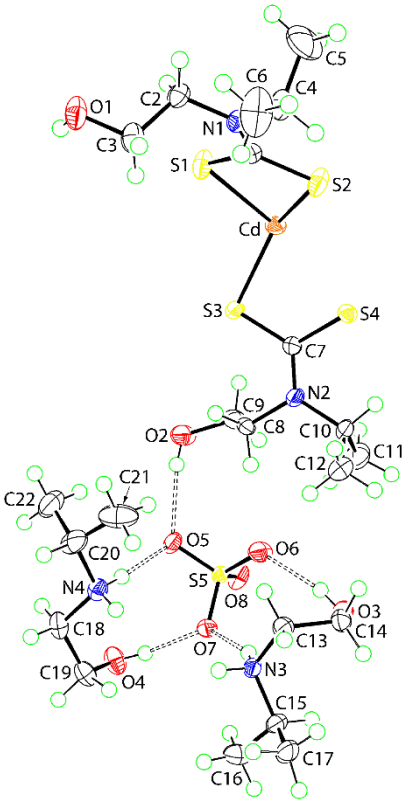

Fig. 11. The asymmetric unit for salt co-crystal **4** showing atom labelling scheme

The key feature of the supramolecular connections between the components of **4** is the formation of chains along the *b*-axis sustained by charge-assisted N–H…O(sulfate) and hydroxyl-O-H···O(sulfate) hydrogen bonds, Fig. 12a and Table 5. The neutral molecules are connected to the chain *via* hydroxyl-O–H…O(ammonium-hydoxyl and sulfate) hydrogen bonds. In this scheme each of the sulfate-O5, O7 and O8 atoms is bifurcated. The result of the aggregation between the chains and neutral molecules is a 3D architecture, Fig. 12b.

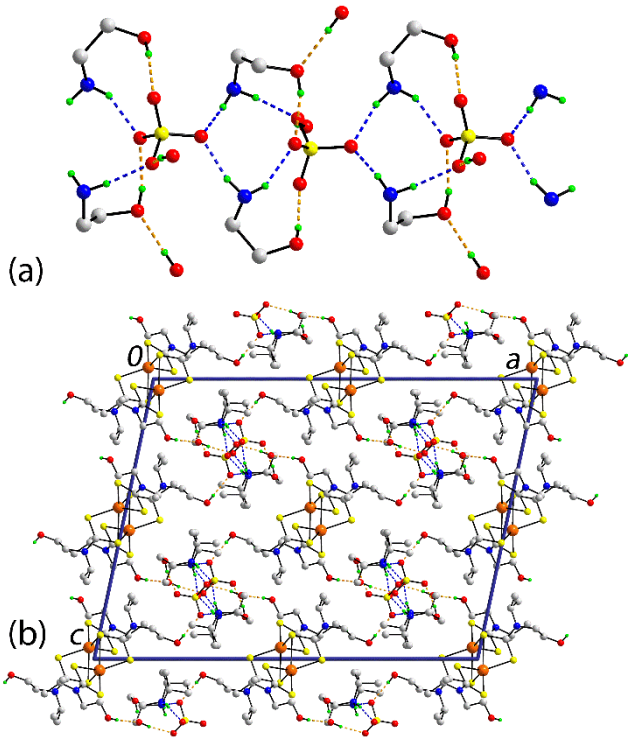

Fig. 12. (a) A view of the supramolecular chain along the *b*-axis sustained by charge-assisted N–H···O(sulfate) (blue dashed lines) and O–H···O(sulfate) hydrogen bonds, and the hydroxyl-O–H···O(hydroxyl) hydrogen bonds (orange) linking the chains to the neutral molecules, and (b) a view of the unit cell contents in projection down the *b*-axis showing the links between the chains of ions and the neutral molecules with non-participating H atoms omitted.

In another attempt to expand the structural landscape of $Cd[S_2CN(iPr)CH_2CH_2OH]_2$, a crystallization reaction between $Cd(acetate)_2.2H_2O$ and two molar equivalents of $Na[S_2CN(iPr)CH_2CH_2OH]$ was attempted in a sodium silicate gel. X-ray crystallography showed the small number of crystals that formed had composition $[iPrNH_2(CH_2CH_2OH)]\{Cd[S_2CN(iPr)CH_2CH_2OH]_3\}$ (**5**). The asymmetric unit comprises a $[iPrNH_2(CH_2CH_2OH)]^+$ cation and a $\{Cd[S_2CN(iPr)CH_2CH_2OH]_3\}^-$ anion, Fig. 13. The Cd atom in the anion is coordinated by three dithiocarbamate ligands and forms a relatively narrow range of Cd–S bond lengths, Table 4, indicating a decidedly more symmetric mode of coordination than observed in **1**–**4**. The coordination geometry is distorted from the ideal octahedral geometry owing to the restricted bite distance of the ligands. The twist angle between the two trigonal faces is estimated to be 38º, compared with 60º in an ideal octahedron, indicating a twist towards a trigonal prismatic geometry. The $\{Cd[S_2CN(iPr)CH_2CH_2OH]_3\}^-$ anion has precedents in the literature being formed when reacting $\{Cd[S_2CNEt_2]_2\}_2$ with aliphatic Lewis bases [99-101].

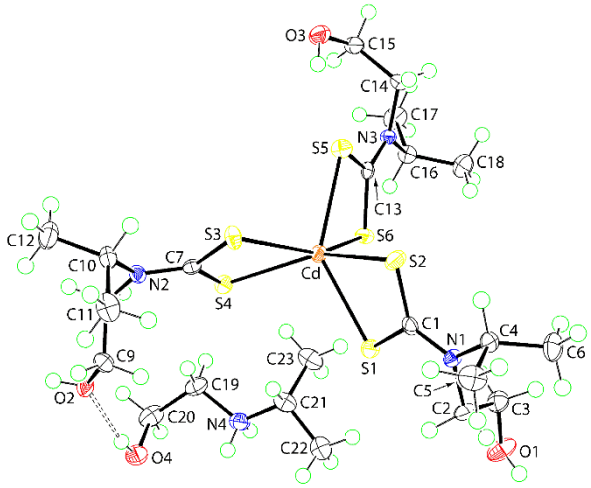

Fig. 13. The symmetric unit for salt **5** showing atom labelling scheme

There are no structurally characterized structures of the cations found in **4** and **5**. As seen from Fig. 14, which presents overlay diagrams for the cations, there is great conformational flexibility in these species with the hydroxyl adopting three very distinct conformations when viewed down the CH_2–CH_2 bond.

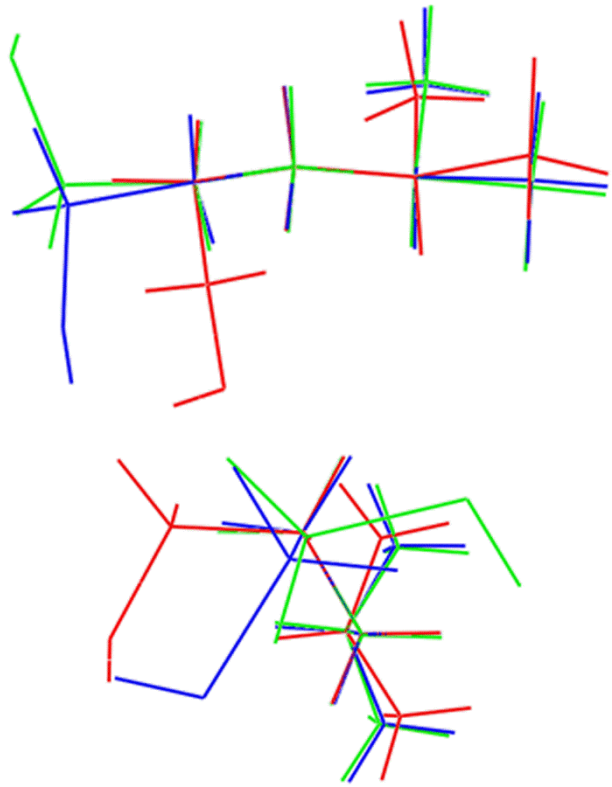

Fig. 14. Two views of the overlay diagram of the cations in **4**, N3-molecule (red image) and inverted-N4-cation (green), and inverted **5** (blue). The cations have been overlapped so that the central C–N–C residues are coincident. In order to ensure the isopropyl groups have the same orientation to highlight the important differences between the conformations, inverted versions of the N4-cation in **4** and the cation in **5** are illustrated. The key torsion angle data quan-

tify the differences in the cations, i.e. N–C–C–O is 48.5(2), -73.6(2) and 59.3(2)º for the N3-cation and N4-cation in **4**, and **5**-cation, respectively. The wide variety in conformations is especially highlighted in the lower image which is a projection down the CH_2CH_2 bonds of the hydroxyethyl groups.

In crystals of **5**, centrosymmetrically related cations associate via charge-assisted N–H···O(hydroxyl) bonds, forming two interactions to the O4 atom. The dimeric aggregates are linked to anions via charge-assisted N–H···O(hydroxyl) and hydroxyl-O–H···O(hydroxyl) hydrogen bonds, Fig. 15a and Table 5. The anions are linked into supramolecular layers in the *ac*-plane by a network of O–H…S hydrogen bonds and incorporating strong C–H···S interactions, Fig. 15b and Table 5. Anionic layers stack along the *b*-axis and are linked into a 3-D structure by the interactions with the interdigitated cationic aggregates, Fig. 15c.

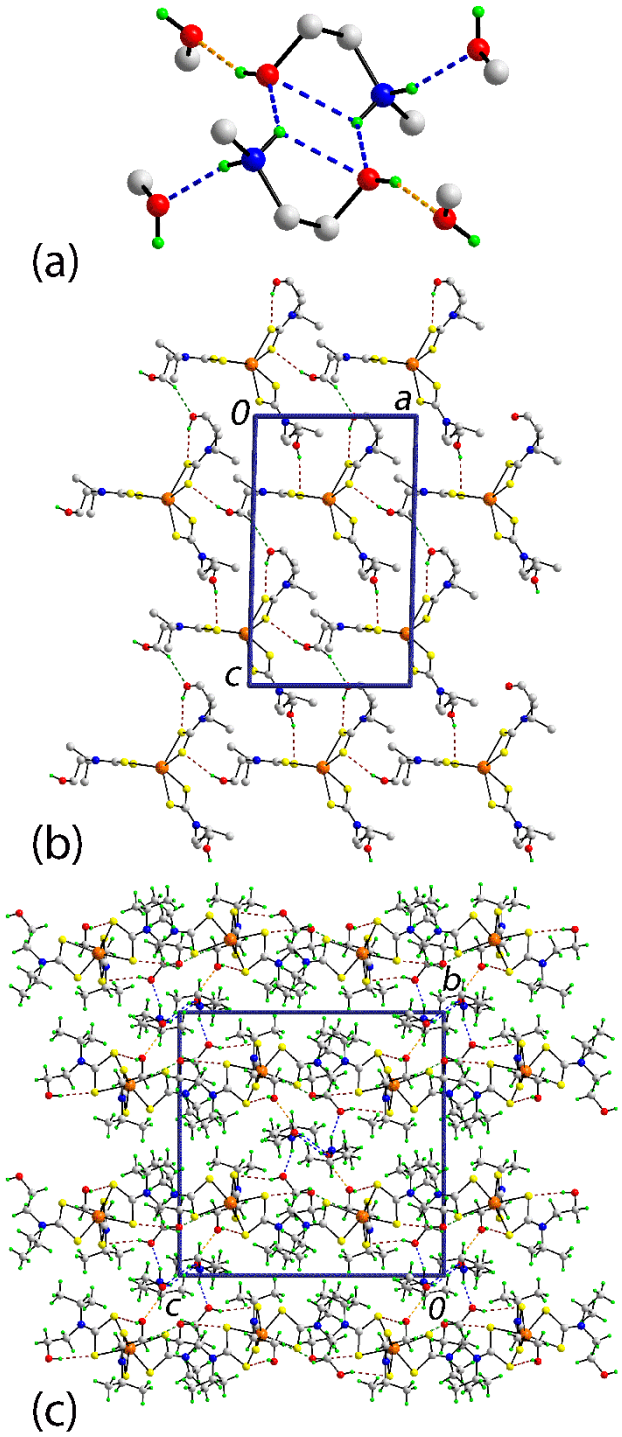

Fig. 15. (a) A view of the bifurcated N–H···O(hydroxyl) hydrogen bonds (blue dashed lines) between atoms and the interaction of these *via* N–H···O(hydroxyl anion) (blue) and hydroxyl-O–H···O(anion hydroxyl) (orange) hydrogen bonds, (b) a view of the supramolecular layer in the *ac*-plane comprising anions connected by O–H···S and incorporating strong C–H···S hydrogen bonding (brown and green dashed lines, respectively) with non-participating H atoms omitted, and (c) a view of the unit cell contents shown in projection down the *a*-axis highlighting the stacking of anionic layers along the *b*-axis being interdigitated by cationic dimeric aggregates.

Conclusions

Needles of coordination polymer $[\{Cd[S_2CN(iPr)CH_2CH_2OH]_2\}\cdot EtOH]_\infty$ (**1**) were isolated within three hours of recrystallization of $Cd[S_2CN(iPr)CH_2CH_2OH]_2$ from ethanol. If the solution is left standing for longer periods the needles transform into blocks which is a genuine SI [54], having the same empirical formula including solvent, being binuclear $\{Cd[S_2CN(iPr)CH_2CH_2OH]_2\}_2\cdot 2EtOH$ (**2**). These results complements the previous characterization "non-genuine" SI, i.e. $[\{Cd[S_2CN(iPr)CH_2CH_2OH]_2\}_3\cdot MeCN]_\infty$ (**6**) and $\{Cd[S_2CN(iPr)CH_2CH_2OH]_2\}_2\cdot 2H_2O\cdot 2MeCN$ (**7**) with the former transforming into the binuclear compound in the presence of water [50]. The initial appearance of the 1-D coordination polymers is correlated with reduced solubility of these species, and the ultimate appearance of the 0-D binuculear species is correlated with it being the thermodynamically more stable, proven in the case of **1** and **2**, and implied in the case of **6** and **7**, solvent mediated transformations between **1**, **2**, **6** and **7**, and the appearance of the binuclear species in 1:2 co-crystal $\{Cd[S_2CN(iPr)CH_2CH_2OH]_2\}_2$:2[3-(propan-2-yl)-1,3-oxazolidine-2-thione] (**3**) and salt co-crystal $[iPrNH_2(CH_2CH_2OH)]_2[SO_4]\{Cd[S_2CN(iPr)CH_2CH_2OH]_2\}_2$ (**4**). In summary, despite the unvaried structural chemistry for the binary cadmium dialkyldithiocarbamates since the report of the first structure in 1968 [31], recent studies [50, 51] indicate that varied crystallization conditions and careful observation can reveal fascinating crystal chemistry for this class of compound.

Acknowledgments

This research was supported by the High Impact Research MoE Grant UM.C/625/1/HIR/MoE/SC/03 from the Ministry of Higher Education, Malaysia.

References

[1] G. Hogarth, *Mini-Rev. Med. Chem.* **2012**, *12*, 1202.
[2] M. Afzaal, M. A. Malik, P. O'Brien, *J. Mater. Chem.* **2010**, *20*, 4031.
[3] D. Coucouvanis, *Prog. Inorg. Chem.* **1979**, *26*, 301.
[4] G. Winter, *Rev. Inorg. Chem.* **1980**, *2*, 253.
[5] W. E. van Zyl, J. D. Woollins, *Coord. Chem. Rev*. **2103**, *257*, 718.
[6] P. J. Heard, *Prog. Inorg. Chem.* **2005**, *53*, 1.
[7] G. Hogarth, *Prog. Inorg. Chem.* **2005**, *53*, 71.
[8] J. Cookson, P. D. Beer, *Dalton Trans*. **2007**, 1459.
[9] E. R. T. Tiekink, I. Haiduc, *Prog. Inorg. Chem.* **2005**, *54*, 127.
[10] I. Haiduc, D. B. Sowerby, *Polyhedron*, **1996**, *15*, 2469.
[11] N. W. Alcock, *Adv. Inorg. Chem. Radiochem*., **1972**, *15*, 1.
[12] I. Haiduc, *Secondary Bonding* in J. L. Atwood, J. Steed, (Eds), *Encyclopedia of Supramolecular Chemistry*, Marcel Dekker Inc., New York, **2004**, pp. 1215.
[13] C. S. Lai, Y. X. Lim, T. C. Yap, E. R. T. Tiekink, *CrystEngComm*, **200**2, *4*, 596.
[14] E. R. T. Tiekink, *CrystEngComm*, **2003**, *5*, 101.
[15] C. S. Lai, E. R. T. Tiekink, *CrystEngComm*, **2003**, *5*, 253.
[16] E. R. T. Tiekink, *CrystEngComm*, **2006**, *8*, 104.
[17] B. F. Abrahams, B. F. Hoskins, E. R. T. Tiekink, G. Winter, *Aust. J. Chem.* **1988**, *41*, 1117.
[18] V. G. Jr. Young, E. R. T. Tiekink, *Acta Crystallogr. Sect. E: Struct. Rep. Online* **2002**, *58*, m537.
[19] H. M. Rietveld, E. N. Maslen, *Acta Crystallogr*. **1965**, *18*, 429.
[20] X.-H. Jiang, W.-G. Zhang, Y. Zhong, F.-X. Wei, S.-L. Wang, *Chin. J. Inorg. Chem.* **2002**, *18*, 615.
[21] Y. Iimura, T. Ito, H. Hagihara, *Acta Crystallogr. Sect. B: Struct. Crystallogr. Cryst. Chem.* **1972**, *28*, 2271.
[22] Y. Iimura, *Sci. Pap. Inst. P. C. R. (Jpn.)* **1973**, *67*, 43.
[23] D. W. Tomlin, T. M. Cooper, D. E. Zelmon, Z. Gebeyehu, J. M. Hughes, *Acta Crystallogr. Sect. C: Cryst. Struct. Commun*. **1999**, *55*, 717.
[24] E. R. T. Tiekink, *Acta Crystallogr. Sect. C: Cryst. Struct. Commun.* **2000**, *56*, 1176.
[25] S. L. Lawton, G. T. Kokotailo, *Inorg. Chem.* **1969**, *8*, 2410.
[26] J. S. Casas, A. Castiñeiras, M. S. Garcia-Tasende, A. Sánchez, J. Sordo, E. M. Vázquez-López, *Polyhedron* **1995**, *14*, 2055.
[27] A. V. Ivanov, O. V. Loseva, M. A. Ivanov, V. A. Konfederatov, A. V. Gerasimenko, O. N. Antsutkin, W. Forsling, *Russ. J. Inorg. Chem*. (Engl. Trans.) **2007**, *52*, 1595.
[28] T. Ito, M. Otake, *Acta Crystallogr. Sect. C: Cryst. Struct. Commun.* **1996**, *52*, 3024.
[29] Y.-G. Yin, W. Forsling, D. Bostrom, O. N. Antzutkin, M. Lindberg, A. Ivanov, *Chin. J. Chem*. **2003**, *21*, 291.
[30] A. V. Ivanov, A. V. Gerasimenko, O. N. Antzutkin, W. Forsling, *Inorg. Chim. Acta*, **2005**, *358*, 2585.
[31] A. Domenicano, L. Torelli, A. Vaciago, L. Zambonelli, *J. Chem. Soc. A*, **1968**, 1351.
[32] E. A. Shugam, V. M. Agre, *Kristallografiya*, **1968**, *13*, 253.
[33] C. M. Dee, E. R. T. Tiekink, *Z. Kristallogr. – New Cryst. Struct.* **2002**, *217*, 85.
[34] A. V. Ivanov, O. V. Loseva, A. V. Gerasimenko, *Koord. Khim.* **2008**, *34*, 413.
[35] D. V. Konarev, A. Yu. Kovalevsky, S. S. Khasanov, G. Saito, D. V. Lopatin, A. V. Umrikhin, A. Otsuka, R. N. Lyubovskaya, *Eur. J. Inorg. Chem.* **2006**, 1881.
[36] E. Jian, Z. Wang, Z. Bai, X. You, H. K. Fun, K. Chinnakali, *J. Chem. Crystallogr.* **1999**, *29*, 227.
[37] A. V. Ivanov, A. A. Konzelko, A. V. Gerasimenko, M. A. Ivanov, O. N. Antsutkin, W. Forsling, *Russ. J. Inorg. Chem*. (Engl. Trans.) **2005**, *50*, 1827.

[38] F.-F. Jian, Z.-X. Wang, H.-K. Fun, Z.-P. Bai, X.-Z. You, *Acta Crystallogr. Sect. C: Cryst. Struct. Commun.* **1999**, *55*, 174.
[39] M. J. Cox, E. R. T. Tiekink, *Z. Kristallogr.* **1999**, *214*, 670.
[40] J. S. Casas, A. Sanchez, J. Bravo, S. Garcia-Fontan, E. E. Castellano, M. M. Jones, *Inorg. Chim. Acta*, **1989**, *158*, 119.
[41] L. A. Glinskaya, S. M. Zemskova, R. F. Klevtsova, *Zh. Strukt. Khim.* **1999**, *40*, 979.
[42] M. Saravanan, K. Ramalingam, G. Bocelli, R. Olla. *Appl. Organomet. Chem.* **2004**, *18*, 103.
[43] X. Yin, W.-G. Zhang, Q.-J. Zhang, J. Fan, C. S. Lai, E. R. T. Tiekink, *Appl. Organomet. Chem.* **2004**, *18*, 139.
[44] Y. Zhong, W. Zhang, J. Fan, M. Tan, C. S. Lai, E. R. T. Tiekink, *Acta Crystallogr. Sect. E: Struct. Rep. Online* **2004**, *60*, m1633.
[45] R. Kant, V. K. Gupta, K. Kapoor, P. Valarmathi, S. Thirumaran, *Acta Crystallogr. Sect. E: Struct. Rep. Online* **2012**, *68*, m12.
[46] A. V. Ivanov, A. V. Gerasimenko, A. A. Konzelko, M. A. Ivanov, O. N. Antzutkin, W. Forsling, *Inorg. Chim. Acta* **2006**, *359*, 3855.
[47] A. Manohar, K. Ramalingam, G. Bocelli, A. Cantoni, *Pol. J. Chem.* **2005**, *79*, 671.
[48] V. M. Agre, E. A. Shugam, *Kristallografiya*, **1972**, *17*, 303.
[49] S. Thirumaran, N. Srinivasan, V. Sharma, V. K. Gupta, Rajnikant, *X-ray. Str. Anal. Online* **2012**, *28*, 21.
[50] Y. S. Tan, A. L. Sudlow, K. C. Molloy, Y. Morishima, K. Fujisawa, W. J. Jackson, W. Henderson, S. N. Bt. A. Halim, S. W. Ng, E. R. T. Tiekink, *Cryst. Growth Des.* **2013**, *13*, 3046.
[51] V. Kumar, V. Singh, A. N. Gupta, K. K. Manar, M. G. B. Drew, N. Singh, *CrystEngComm*, **2014**, *16*, 6765.
[52] L. H. van Poppel, T. L. Groy, M. T. Caudle, *Inorg. Chem.* **2004**, *43*, 3180.
[53] B. Moulton, M. J. Zaworotko, *Chem. Rev.* **2001**, *101*, 1629.
[54] J.-P. Zhang, X.-C. Huang, X.-M. Chen, *Chem. Soc. Rev.* **2009**, *38*, 2385.
[55] L. Dobrzańska, *Inorg. Chem. Commun.* **2015**, *55*, 21.
[56] C.-P. Li, M. Du *Chem. Commun.* **2011**, *47*, 5958.
[57] A. M. P. Peedikakkal, J. J. Vittal, *Cryst. Growth Des.* **2011**, *11*, 4697.
[58] D. Frahm, F. Hoffmann, M. Fröba, *Cryst. Growth Des.* **2014**, *14*, 1719.
[59] S.-H. Li, M.-L. Han, G.-Z. Liu, L.-F. Ma, L.-Y. Wang, *RSC Adv.* **2015**, *5*, 17588.
[60] L.-L. Han, T.-P. Hu, K. Mei, Z.-M. Guo, C. Yin, Y.-X. Wang, J. Zheng, X. -P. Wang, D. Sun, *Dalton Trans.* **2015**, *44*, 6052.
[61] B. Manna, S. Singh, A. Karmakar, A. V. Desai, S. K. Ghosh, *Inorg. Chem.* **2015**, *54*, 110.
[62] D. Sun, Y. Ke, T. M. Mattox, B. A. Ooro, H. -C. Zhou, *Chem. Commun.* **2005**, 5447.
[63] S. S. Nagarkar, A. K. Chaudhari, S. K. Ghosh, *Cryst. Growth Des.* **2012**, *12*, 572.
[64] B. Liu, L.-Y. Pang, L. Hou, Y.-Y. Wang, Y. Zhang, Q.-Z. Shi, *CrystEngComm*, **2012**, *14*, 6246.
[65] S. Wang, Y. Peng, X. Wei, Q. Zhang, D. Wang, J. Dou, D. Lia, J. Bai, *CrystEngComm*, **2011**, *13*, 5313.
[66] M. du Plessis, L. J. Barbour, *Dalton Trans.* **2012**, *41*, 3895.
[67] X. Meng, X.-Z. Song, S.-Y. Song, S.-Q. Su, M. Zhu, Z.-M. Hao, S.-N. Zhao, H.-J. Zhang, *Dalton Trans.* **2013**, *42*, 5619.
[68] S.-S. Hou, X. Huang, J.-G. Guo, S. -R. Zheng, J. Lei, J.-B. Tan, J. Fan, W.-G. Zhang, *CrystEngComm*, **2015**, *17*, 947.
[69] Q. Xia, Y. Ren, M.-L. Cheng, X. Liu, S. Chen, C. Zhai, Q. Liu, *J. Coord. Chem.* **2015**, *68*, 1688.
[70] D.-S. Chen, L.-B. Sun, Z.-Q. Liang, K.-Z. Shao, C.-G. Wang, Z.-M. Su, H.-Z. Xing, *Cryst. Growth Des.* **2013**, *13*, 4092.

[71] E. Lee J.-Y. Kim, S. S. Lee, K.-M. Park, *Chem. Eur. J.* **2013**, *19*, 13638.
[72] A. B. Lago, R. Carballo, S. Rodríguez-Hermida, E. M. Vázquez-López, *CrystEngComm*, **2013**, *15*, 1563.
[73] S.-W. An, L. Mei, C.-Z. Wang, C.-Q. Xia, Z.-F. Chai, W.-Q. Shi, *Chem. Commun*. **2015**, *51*, 8978.
[74] P. Poplaukhin, E. R. T. Tiekink, *CrystEngComm*, **2010**, *12*, 1302.
[75] I. Rojas-León, J. A. Guerrero-Alvarez, J. Hernández-Paredes, H. Höpfl, *Chem. Commun*. **2012**, *48*, 401.
[76] P. Poplaukhin, H. D. Arman, E. R. T. Tiekink, *Z. Kristallogr*. **2012**, *227*, 363.
[77] G. M. Sheldrick, SADABS. University of Göttingen, Germany, **1996**.
[78] *CrysAlis PRO*. Agilent Technologies, Yarnton, Oxfordshire, England, **2011**.
[79] G. M. Sheldrick, *Acta Cryst. Sect. A: Found. Crystallogr*. **2008**, *64*, 112.
[80] G. M. Sheldrick, *Acta Cryst. Sect. C: Cryst. Struct. Commun*. **2015**, *71*, 3.
[81] L. J. Farrugia, *J. Appl. Crystallogr*. **2012**, *45*, 849.
[82] K. Brandenburg, DIAMOND. Crystal Impact GbR, Bonn, Germany, **2006**.
[83] J. Gans, D. Shalloway, *J. Molec. Graphics Model*. **2001**, *19*, 557.
[84] X'Pert HighScore Plus. PANalytical B.V., Almelo, The Netherlands, **2009**.
[85] L. A. Dubraja, D. Matković-Čalogović, P. Planinić, *CrystEngComm*, **2015**, *17*, 2021.
[86] A. W. Addison, T. N. Rao, J. Reedijk, J. van Rijn, G. C. Verschoor, *J. Chem. Soc. Dalton Trans*. **1984**, 1349.
[87] S. Mlowe, D. J. Lewis, M. A. Azad, J. Raftery, E. B. Mubofu, P. O'Brien, N. Revaprasadu, *New J. Chem*. **2014**, *38*, 6073.
[88] M. A. Ehsan, H. N. Ming, M. Misran, Z. Arifin, E. R. T. Tiekink, A. P. Safwan, M. Ebadi, W. J. Basirun, M. Mazhar, *Chem. Vap. Deposition* **2012**, *18*, 191.
[89] J. J. Vittal, *Coord. Chem. Rev*. **2007**, *251*, 1781.
[90] I.-H. Park, S. S. Lee, J. J. Vittal, *Chem. Eur. J*. **2013**, *19*, 2695.
[91] B. Liu, L.-Y. Pang, L. Hou, Y.-Y. Wang, Y. Zhang, Q.-Z. Shi, *CrystEngComm*, **2012**, *14*, 6246.
[92] Y. Jeon, S. Cheon, S. Cho, K. Y. Lee, T. H. Kim, J. Kim, J. *Cryst. Growth Des*. **2014**, *14*, 2105.
[93] G. Li, C. Wang, X. Zhang, *J. Coord. Chem*. **2013**, *66*, 1107.
[94] G.-D. Zou, Z.-Z. He, C.-B. Tian, L.-J. Zhou, M.-L. Feng, X.-D. Zhang, X.-Y. Huang, *Cryst. Growth Des.* **2014**, *14*, 4430.
[95] Y. S. Tan, S. N. A. Halim, E. R. T. Tiekink, *Z. Kristallogr. – New Cryst. Struct*. **2014**, *229*, 55.
[96] R. Nomura, M. Kori, H. Matsuda, *Chem. Lett*. **1985**, 579.
[97] R. Mothes, A. Jakob, T. Waechtler, S. E. Schulz, T. Gessner, H. Lang, *Eur. J. Inorg. Chem*. **2015**, 1726.
[98] C. R. Groom, F. H. Allen, *Angew. Chem. Int. Ed*. **2014**, *53*, 662.
[99] J. McCleverty, S. Gill, R. S. Z. Kowalski, N. A. Bailey, H. Adams, K. W. Lumbard, M. A. Murphy, *J. Chem. Soc., Dalton Trans*. **1982**, 493.
[100] L. A. Glinskaya, S. M. Zemskova, R. F. Klevtsova, S. V. Larinov, S. A. Gromilov, *Polyhedron*, **1992**, *11*, 2951.
[101] S. M. Zemskova, L. A. Glinskaya, R. F. Klevtsova, M. A. Fedotov, S. V. Larinov, *J. Struct. Chem*. **1999**, *40*, 284.

Exploring the crystallization landscape of cadmium bis(*N*-hydroxyethyl, *N*-isopropyldithiocarbamate), $Cd[S_2CN(iPr)CH_2CH_2OH]_2$

Yee Seng Tan,[I] Siti Nadiah Abdul Halim[I] and Edward R. T. Tiekink*[I,II]

[I] University of Malaya, Department of Chemistry, 50603 Kuala Lumpur, Malaysia

[II] Sunway University, Centre for Chemical Crystallography, Faculty of Science and Technology, 47500 Bandar Sunway, Selangor Darul Ehsan, Malaysia

******* SUPPLEMENTARY MATERIAL *******

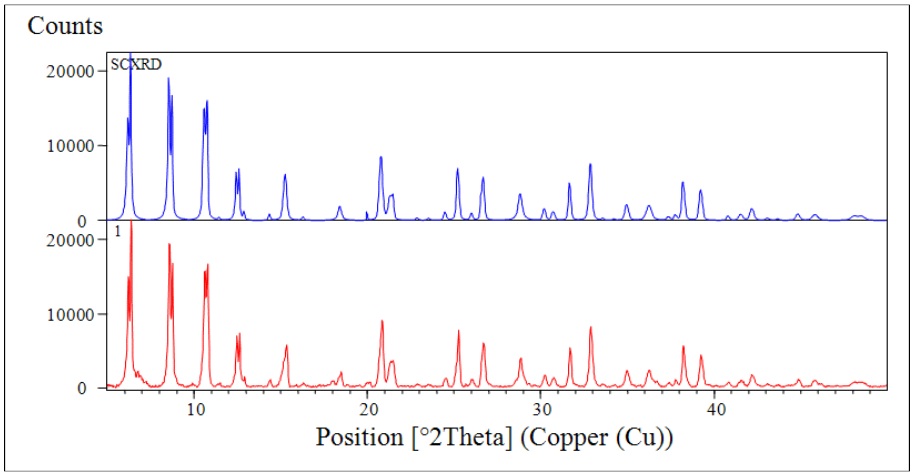

(a)

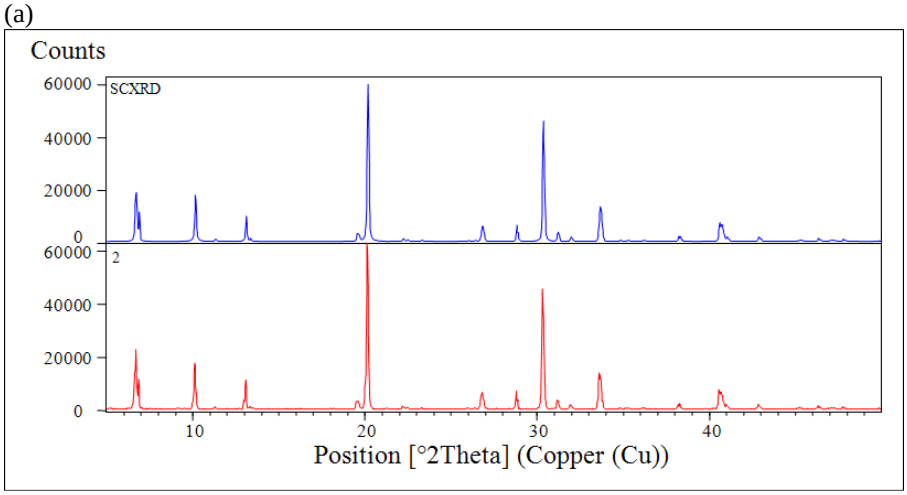

(b)

Figure S1. Experimental (red trace) and calculated (blue) PXRD patterns for **1** (a), and **2** (b).

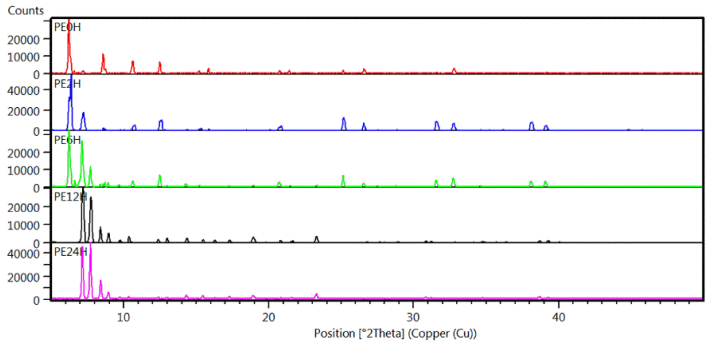

(a)

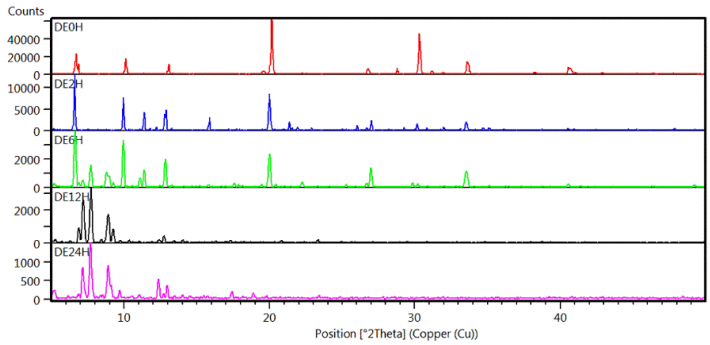

(b)

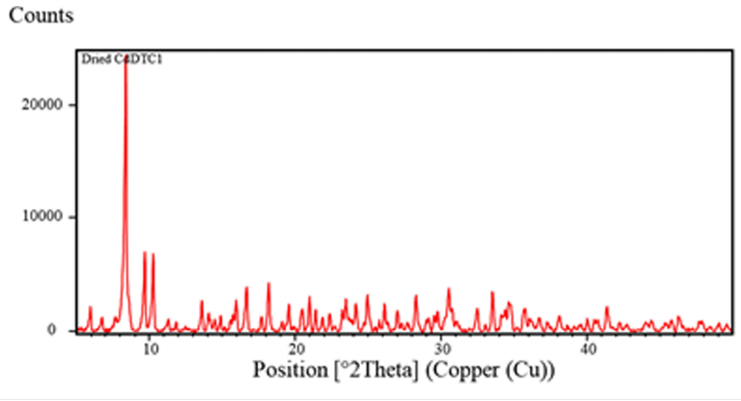

(c)

Figure S2. Time-dependent PXRD patterns for **1** (a) and **2** (b) measured at 0 h (red traces), 2 h (blue), 6 h (green), 12 h (black) and 24 (purple). These indicate changes in crystal structure occurred before 2 h in each case. PXRD pattern for $Cd[S_2CN(iPr)CH_2CH_2OH]_2$, the starting material used for recrystallization (c).

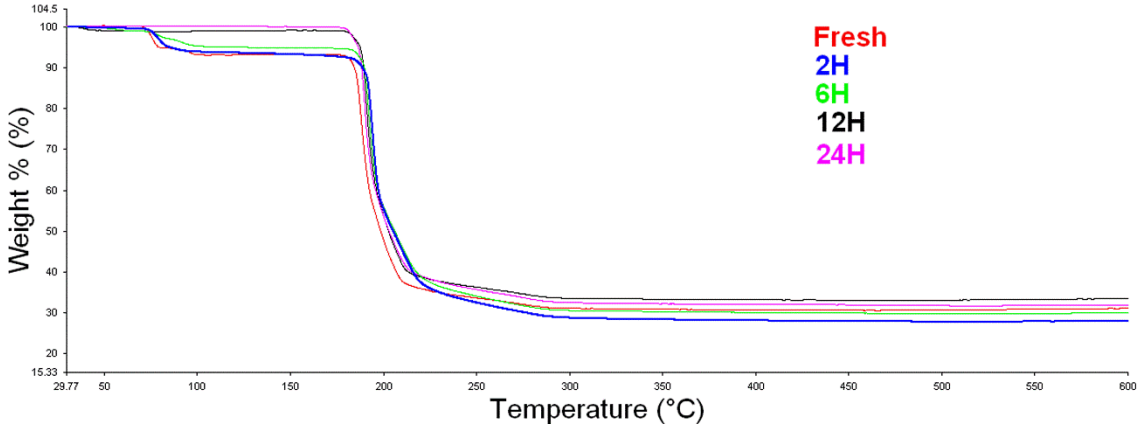

(a)

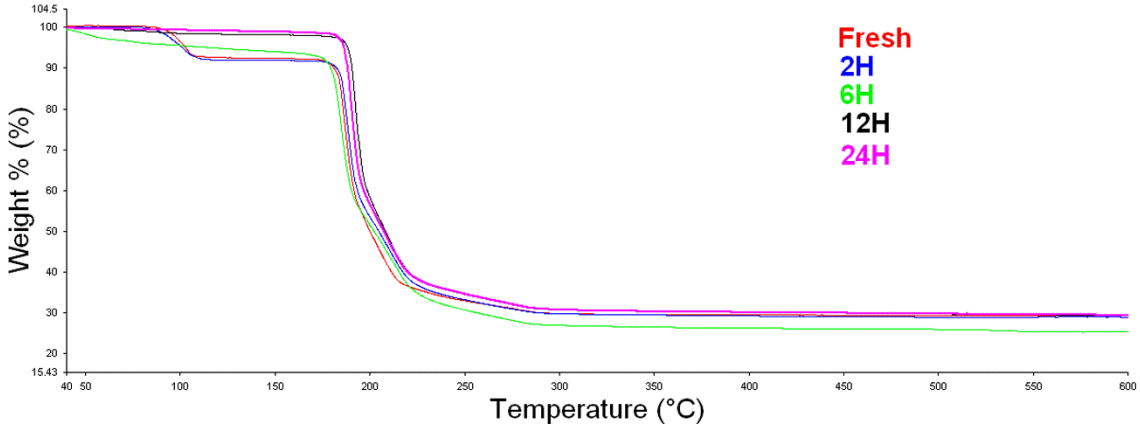

(b)

Figure S3. Time-dependent TGA measurements for **1** (a) and **2** (b), showing the samples had lost most of the ethanol of crystallization after 6 h.

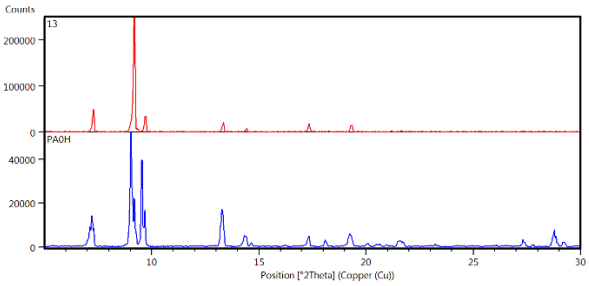
Counts
13
PA0H
Position [°2Theta] (Copper (Cu))

(a)

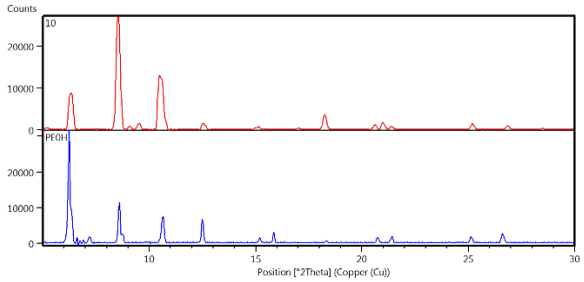
Counts
10
PE0H
Position [°2Theta] (Copper (Cu))

(b)

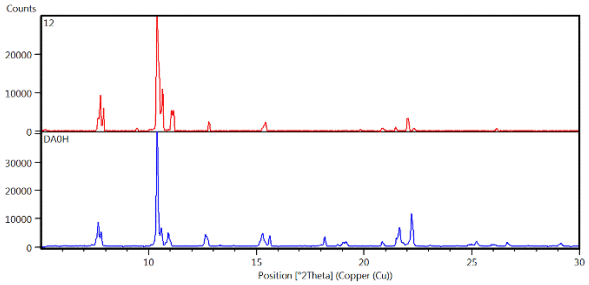
Counts
12
DA0H
Position [°2Theta] (Copper (Cu))

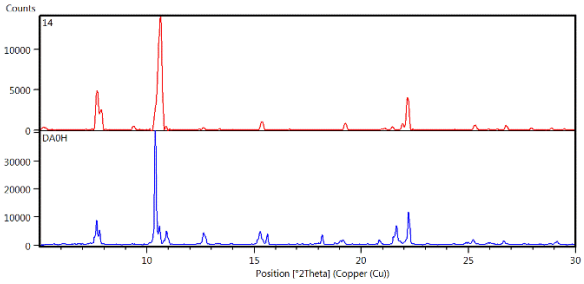
Counts
14
DA0H
Position [°2Theta] (Copper (Cu))

(c)

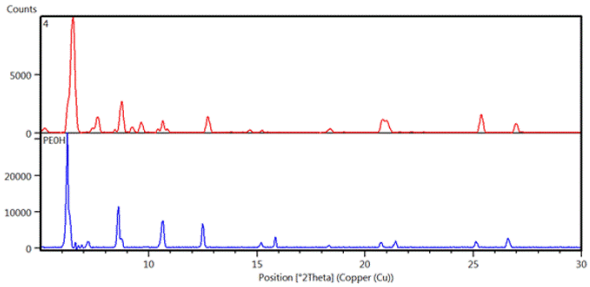
Counts
4
PE0H
Position [°2Theta] (Copper (Cu))

(d)

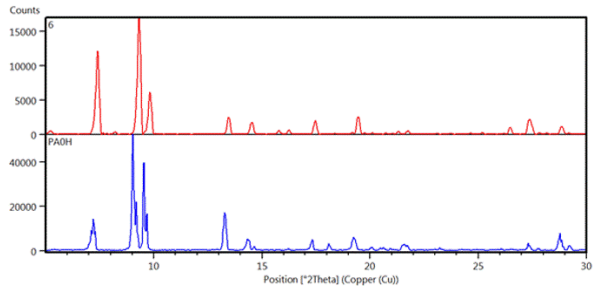

(e)

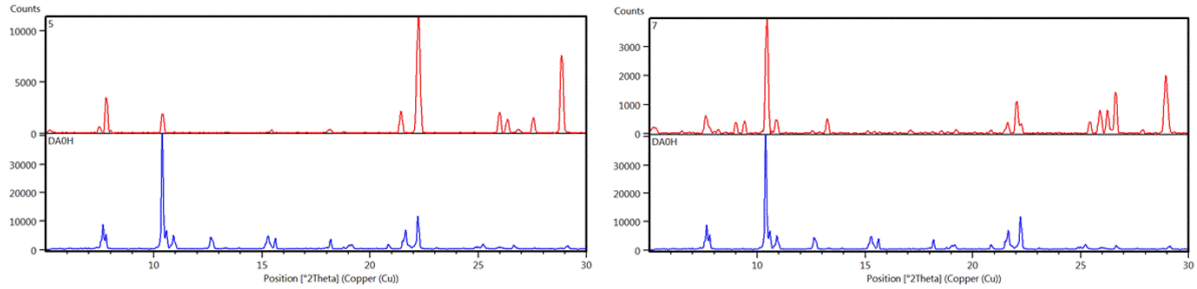

(f)

Figure S4. PXRD for solvent mediated transformations of SI. PXRD showing the formation of **6** from recrystallization of **1** from dry MeCN in a desiccator (a). **1** from **6**: Dry EtOH, dessicator (b). **7** from **1**: Ambient, left – dry MeCN and right – laboratory grade MeCN, (c). **1** from **7**: Ambient, laboratory grade EtOH; the small extra peaks are due to original **7** (d). **6** from **2**: dry MeCN, desiccator (e). **7** from **2**: Ambient, left – dry MeCN and right – laboratory grade MeCN; the small extra peaks in the right-hand image are due to an unidentified species (f). The top (red) trace is of the product of the recrystallization and the bottom (blue) trace is of an authenticated sample.